ADVANCING EARTH AND SPACE SCIENCES

Water Resources Research

RESEARCH ARTICLE
10.1029/2023WR034794

Synchrony of Nitrogen Wet Deposition Inputs and Watershed Nitrogen Outputs Using Information Theory

Desneiges S. Murray[1], Edom Moges[2], Laurel Larsen[2], Michelle D. Shattuck[1], William H. McDowell[1], and Adam S. Wymore[1]

[1]Department of Natural Resources and the Environment, University of New Hampshire, Durham, NH, USA, [2]Department of Geography, University of California, Berkeley, Berkeley, CA, USA

Key Points:

- Wet deposition-river N synchrony was resolved at timescales greater than hydrologic processes such as surface flow runoff
- The timing of peak synchrony indicates that N deposition may magnify processes like assimilation and mineralization in the watershed
- While deposition N contributed information to river N, the magnitude suggests sources besides wet deposition are driving river N

Supporting Information:

Supporting Information may be found in the online version of this article.

Correspondence to:

D. S. Murray,
desneiges.murray@unh.edu

Citation:

Murray, D. S., Moges, E., Larsen, L., Shattuck, M. D., McDowell, W. H., & Wymore, A. S. (2023). Synchrony of nitrogen wet deposition inputs and watershed nitrogen outputs using information theory. *Water Resources Research*, *59*, e2023WR034794. https://doi.org/10.1029/2023WR034794

Received 2 MAR 2023
Accepted 7 OCT 2023

Author Contributions:

Conceptualization: Desneiges S. Murray, Laurel Larsen, Adam S. Wymore
Data curation: Desneiges S. Murray, Michelle D. Shattuck, William H. McDowell
Formal analysis: Desneiges S. Murray
Funding acquisition: Desneiges S. Murray, William H. McDowell, Adam S. Wymore
Investigation: Desneiges S. Murray
Methodology: Desneiges S. Murray, Edom Moges, Laurel Larsen
Project Administration: Michelle D. Shattuck, William H. McDowell, Adam S. Wymore
Resources: Desneiges S. Murray, Laurel Larsen, William H. McDowell, Adam S. Wymore

Abstract

Nitrogen (N) wet deposition chemistry impacts watershed biogeochemical cycling. The timescale and magnitude of (a)synchrony between wet deposition N inputs and watershed N outputs remains unresolved. We quantify deposition-river N (a)synchrony with transfer entropy (TE), an information theory metric enabling quantification of lag-dependent feedbacks in a hydrologic system by calculating directional information flow between variables. Synchrony is defined as a significant amount of TE-calculated reduction in uncertainty of river N from wet deposition N after conditioning for antecedent river N conditions. Using long-term timeseries of wet deposition and river DON, NO_3^-, and NH_4^+ concentrations from the Lamprey River watershed, New Hampshire (USA), we constrain the role of wet deposition N to watershed biogeochemistry. Wet deposition N contributed information to river N at timescales greater than quick-flow runoff generation, indicating that river N losses are a lagged non-linear function of hydro-biogeochemical forcings. River DON received the most information from all three wet deposition N solutes while wet deposition DON and NH_4^+ contributed the most information to all three river N solutes. Information theoretic algorithms facilitated data-driven inferences on the hydro-biogeochemical processes influencing the fate of N wet deposition. For example, signals of mineralization and assimilation at a timescale of 12 to 21-weeks lag display greater synchrony than nitrification, and we find that N assimilation is a positive lagged function of increasing N wet deposition. Although wet deposition N is not the main driver of river N, it contributes a significant amount of information resolvable at time scales of transport and transformations.

Plain Language Summary

Nitrogen (N) dissolved within precipitation (e.g., wet deposition) is an important input of N from the atmosphere to biosphere. Whether wet deposition N is synchronized with watershed biogeochemical processes, including N losses to rivers, remains unresolved at fine temporal scales. Synchrony is a phenomenon observed between variables displaying complex interactions with potentially lagged temporal relationships. Information theory algorithms, like transfer entropy (TE), quantify directional information flow between variables, enabling the quantification of lag-dependencies and feedback cycles in a hydrologic system, informative for creating conceptual models of watershed-scale biogeochemical processes. Here, wet deposition-river N synchrony between pair-wise combinations of dissolved organic N, NO_3^-, and NH_4^+ is expressed as the timing and magnitude of TE at the same time step or pre-determined lag. Synchrony was calculated using 17-years of weekly paired wet deposition-river N observations from the Lamprey River watershed. Precipitation and streamflow were most synchronized at no lag, while biogeochemical analyses were synchronized at lags between 12 and 21-weeks, indicating N losses are a function of hydrologic and biogeochemical forcings. We quantified strength and timing of synchrony for each pair of N solutes. Signals of inorganic and organic N incorporation into biomass and conversion of organic N to inorganic N displayed the greatest synchrony, suggesting that N wet deposition inputs may contribute to uptake and further cycling of N within terrestrial and aquatic biomass.

1. Introduction

Dissolved nitrogen (N) entering an ecosystem through wet deposition (e.g., precipitation) is subject to many fates driven by a watershed's hydrology (Burt & McDonnell, 2015) and capacity for solute biogeochemical processing (Aber et al., 1998; Monteith et al., 2023). Wet deposition N, including nitrate (NO_3^-), ammonium (NH_4^+), and dissolved organic N (DON), can be immediately discharged to rivers via surface and sub-surface flow paths during storm events (Baron et al., 2013; Kirker & Toran, 2023; Whitehead et al., 2009), temporarily stored in saturated soil pore water (Bastviken et al., 2006; Dunne, 1978), exchanged within soil clay minerals (Robertson

Software: Desneiges S. Murray, Edom Moges, Laurel Larsen
Supervision: Laurel Larsen, William H. McDowell, Adam S. Wymore
Validation: Desneiges S. Murray, Edom Moges, Laurel Larsen
Visualization: Desneiges S. Murray
Writing – original draft: Desneiges S. Murray
Writing – review & editing: Desneiges S. Murray, Edom Moges, Laurel Larsen, Michelle D. Shattuck, William H. McDowell, Adam S. Wymore

et al., 1999), and subjected to plant uptake (Bernal et al., 2012; Lovett et al., 2000) or to microbially mediated biogeochemical transformations (Jenkinson et al., 1985). The biogeochemical fate of wet deposition N also depends on its form. For example, DON can be mineralized, NH_4^+ can be nitrified, and DON, NH_4^+, and NO_3^- can be assimilated. Dissolved N cycled through watershed transient storage zones can ultimately contribute to the chemical load in receiving stream water (Boyer et al., 1997; Chorover et al., 2017; Hornberger et al., 1994, 2001). While wet deposition chemistry can impart significant long-term influence on surface water chemistry (Aber et al., 2003; Monteith et al., 2007; Murdoch & Stoddard, 1992; Newcomer et al., 2021; Templer et al., 2022), the timescales over which wet deposition N inputs are related to watershed N outputs remain unresolved. As reactive N deposition inputs change in concentration and stoichiometry due to emission policies like the Clean Air Act (Gilliam et al., 2019; Murray et al., 2022), determining the magnitude to which N wet deposition contributes to river N losses is important for managing excess N loading to receiving waterbodies.

Watershed N losses via surface water are a product of non-linear, dynamic interactions between the atmosphere, terrestrial environment, and watershed hydrology (Brookshire et al., 2007). Existing quantitative and experimental methods, however, provide a limited understanding of the prevalence of these non-linear mechanisms driving (a)synchronous relationships between wet deposition inputs and watershed outputs. Correlative model structures are commonly used to evaluate biogeochemical timeseries data. While such approaches are useful for conveying linear relationships between inputs and outputs (Argerich et al., 2013; Halliday et al., 2013; Rodríguez-Cardona et al., 2022), they provide limited insights into mechanisms and time lags that underlie the dynamics and interdependencies between environmental timeseries, particularly those that are not linear (Runge et al., 2019). Experimental approaches are informative for describing the mechanisms that facilitate biogeochemical processing of N deposition but limited in other ways. For example, chamber experiments or ex situ sediment core methods are representative of plot or reach-scale spatial-temporal conditions (e.g., McDowell et al., 2004) but are labor-intensive and do not capture an integrative picture of biogeochemical processes and environmental conditions at the watershed scale. On the other hand, earth-system or process-based models of watershed biogeochemical cycling (e.g., Byrnes et al., 2020; Neitsch et al., 2001; Parton, 1996; Smith et al., 1997) impose strong mechanistic assumptions about catchment and ecosystem-scale processes that may not apply uniformly across spatiotemporal scales (Monteith et al., 2023). An alternative set of methods that capture the (a)synchrony between wet deposition inputs and watershed outputs is needed to resolve the range of biotic and abiotic transformations to which atmospherically deposited N is subjected before reaching a stream.

Increasing access to long-term timeseries from the land-atmosphere interface provides opportunities to identify (a)synchronous behaviors of watershed N inputs and outputs. Here we view synchrony as the embodiment of both linear and complex non-linear interactions that lead to high spatiotemporal coherence and consistent lagged behavior through time (Seybold, Fork, et al., 2022). Thus, (a)synchrony cannot be quantified based only on linear metrics. Alternatively, (a)synchrony can be assessed through information theory metrics, which can quantify the amount, lag time, and persistence of information transfer (Feng et al., 2019) from a source variable (e.g., wet deposition N) to a sink variable (e.g., river N). In addition to robustly resolving nonlinear relationships without assumptions of a functional form (Ruddell & Kumar, 2009), information theory metrics like transfer entropy (TE) can account for the influence of antecedent conditions in the sink variable. Within the framework of information theory, synchrony can be quantified as the percent reduction in uncertainty that is achieved in predicting the sink variable given knowledge of the source variable at the same time step or at a pre-determined lag, conditioned on the antecedent value of the sink variable. By providing a means to quantify directional information flows among variables, information theory can support inference of biogeochemical mechanisms in a hydrologic system (Franzen et al., 2020; Moges, Ruddell, Zhang, Driscoll, & Larsen, 2022; Tennant et al., 2020). Here, we present a novel application of information theory in which we use TE to detect synchrony between watershed N inputs (i.e., via wet deposition) and outputs (i.e., via streamflow).

Information theory has origins in statistics and engineering (Shannon, 1949) but has been successfully applied to understanding information transfer between wind speed, temperature and relative humidity (Goodwell & Kumar, 2017), precipitation and discharge (Bennett et al., 2019; Franzen et al., 2020; Moges, Ruddell, Zhang, Driscoll, & Larsen, 2022), methane evasion and water levels in wetlands (Sturtevant et al., 2016), as well as timescales of information exchange between dominant processes influencing stream metabolism (Larsen & Harvey, 2017). Transfer entropy is grounded in mutual information (MI) and Shannon entropy (H(X)). MI has been used as an ancillary method to quantify the covariation between stream solute concentrations (Ardón et al., 2013; Rodríguez-Cardona et al., 2022) and with other environmental factors (Ardón et al., 2017). Here we use TE, over MI, to reflect the (a)synchrony between two timeseries because TE can condition source-to-sink information transfer on antecedent conditions in the sink variable.

Shannon entropy is a measure of the variable's information content—or the variable's inherent uncertainty—and is based on variable *X*'s probability distribution ($p(x)$). In discretized form, $H(X)$ can be expressed as:

$$H(X) = -\sum_{x \in X} p(x) \log(p(x)) \tag{1}$$

Variables with uniformly distributed values have the maximum possible $H(X)$ (equal to the log of the number of bins used for a discretized probability distribution), while variables with only one possible value have a $H(X)$ of zero. Analogously, MI, or amount of overlapping information between two variables (e.g., *X* and *Y*), can be computed from the joint and marginal probability distributions of the variables:

$$\mathrm{MI}(X, Y) = \sum_{x} \sum_{y} p(x, y) \log \frac{p(x, y)}{p(x)p(y)} \tag{2}$$

MI is symmetric, with a minimum value of 0 bits and a maximum value of the min($H(X)$, $H(Y)$). MI can be thought of as the reduction in uncertainty of *X* given knowledge of *Y*, or vice-versa. The MI between two random variables can also be conditioned on a third variable—the history of the "sink" variable (e.g., *Y*)—resulting in directional information flow expressed as TE (or conditional mutual information). TE represents the reduction of uncertainty in the sink variable from the source variable once the history of the sink variable has been accounted for (Schreiber, 2000). Following Ruddell and Kumar (2009), TE can be expressed as:

$$\mathrm{TE}_{X \to Y} = \sum_{Y_t, Y_{t-\Delta t}, X_{t-\tau}} p(Y_t, Y_{t-\Delta t}, X_{t-\tau}) * \log\left(\frac{p(Y_t | Y_{t-\Delta t}, X_{t-\tau})}{p(Y_t | Y_{t-\Delta t})}\right) \tag{3}$$

where t represents the current time, Δt is the sample interval (i.e., temporal resolution of the timeseries), and τ is the lag time between the source and sink variable. Here, $Y_{t-\Delta t}$ is the value of *Y* at the previous timestep and is an appropriate representation of the history of the sink variable for finite-length data sets (Knuth et al., 2013; Ruddell & Kumar, 2009; Wibral et al., 2013). TE is both asymmetric and directional, which supports its use for mechanistic inference (Goodwell & Kumar, 2017; Moges, Ruddell, Zhang, Driscoll, & Larsen, 2022; Rinderer et al., 2018). Here, TE represents additional information contributed to the future state of river discharge or chemistry by knowledge of precipitation volume or wet deposition chemistry. In an applied context, TE uncertainty reduction can be thought of as the strength of deposition timeseries to be a predictive variable for river chemistry timeseries. This metric can inform inferences on the dominant mechanisms determining river chemistry to include in other models or data collection priorities in a given watershed.

We applied information theory analyses to 17-years of paired timeseries of the three most abundant forms of dissolved N: DON, NH_4^+, NO_3^- for wet deposition N (source variable) and river N (sink variable). Information transfer from wet deposition to river timeseries, after accounting for river N history, is expressed as $\mathrm{TE}_{\mathrm{deposition} \to \mathrm{river}}$. The timing of $\mathrm{TE}_{\mathrm{deposition} \to \mathrm{river},}$ or $\mathrm{TE}_{\mathrm{timing}}$, is the time lag(s) ($\tau$) at which statistically significant information transfer occurred between the two timeseries (Figure 1a). Beyond its statistical definition, significant $\mathrm{TE}_{\mathrm{deposition} \to \mathrm{river}}$ can suggest the magnitude of resolvable synchrony (i.e., detectable information transfer based on the algorithm's capabilities) between wet deposition N and river N, and $\mathrm{TE}_{\mathrm{timing}}$ provides insight into the timescales over which hydro-biogeochemical mechanisms may be controlling watershed N losses. Because synchrony between timeseries may occur at a consistent lag (Seybold, Fork, et al., 2022), we interpret peak $\mathrm{TE}_{\mathrm{timing}}$ as the lag at which the source variable is consistently (or repeatedly) reducing uncertainty in the sink variable the most across all timesteps.

We use TE to quantify conditional information flow from precipitation depth to discharge depth, which serves as a null analysis accounting for hydrological synchrony alone, and concentrations of wet deposition N inputs to river N outputs for the same N species (e.g., $NO_3^-{}_{\mathrm{deposition}} \times NO_3^-{}_{\mathrm{river}}$, $NH_4^+{}_{\mathrm{deposition}} \times NH_4^+{}_{\mathrm{river}}$, $\mathrm{DON}_{\mathrm{deposition}} \times \mathrm{DON}_{\mathrm{river}}$) and for all pair-wise combinations of N species that follow primary transformations in the N cycle (e.g., $NH_4^+{}_{\mathrm{deposition}} \times NO_3^-{}_{\mathrm{river}}$, $NH_4^+{}_{\mathrm{deposition}} \times \mathrm{DON}_{\mathrm{river}}$, $NO_3^-{}_{\mathrm{deposition}} \times \mathrm{DON}_{\mathrm{river}}$, $\mathrm{DON}_{\mathrm{deposition}} \times NO_3^-{}_{\mathrm{river}}$, $\mathrm{DON}_{\mathrm{deposition}} \times NH_4^+{}_{\mathrm{river}}$). Pair-wise analyses were classified into five N cycle reaction categories: mineralization (e.g., organic to inorganic), assimilation (inorganic to organic), nitrification (NH_4^+ to NO_3^-), closed-loop

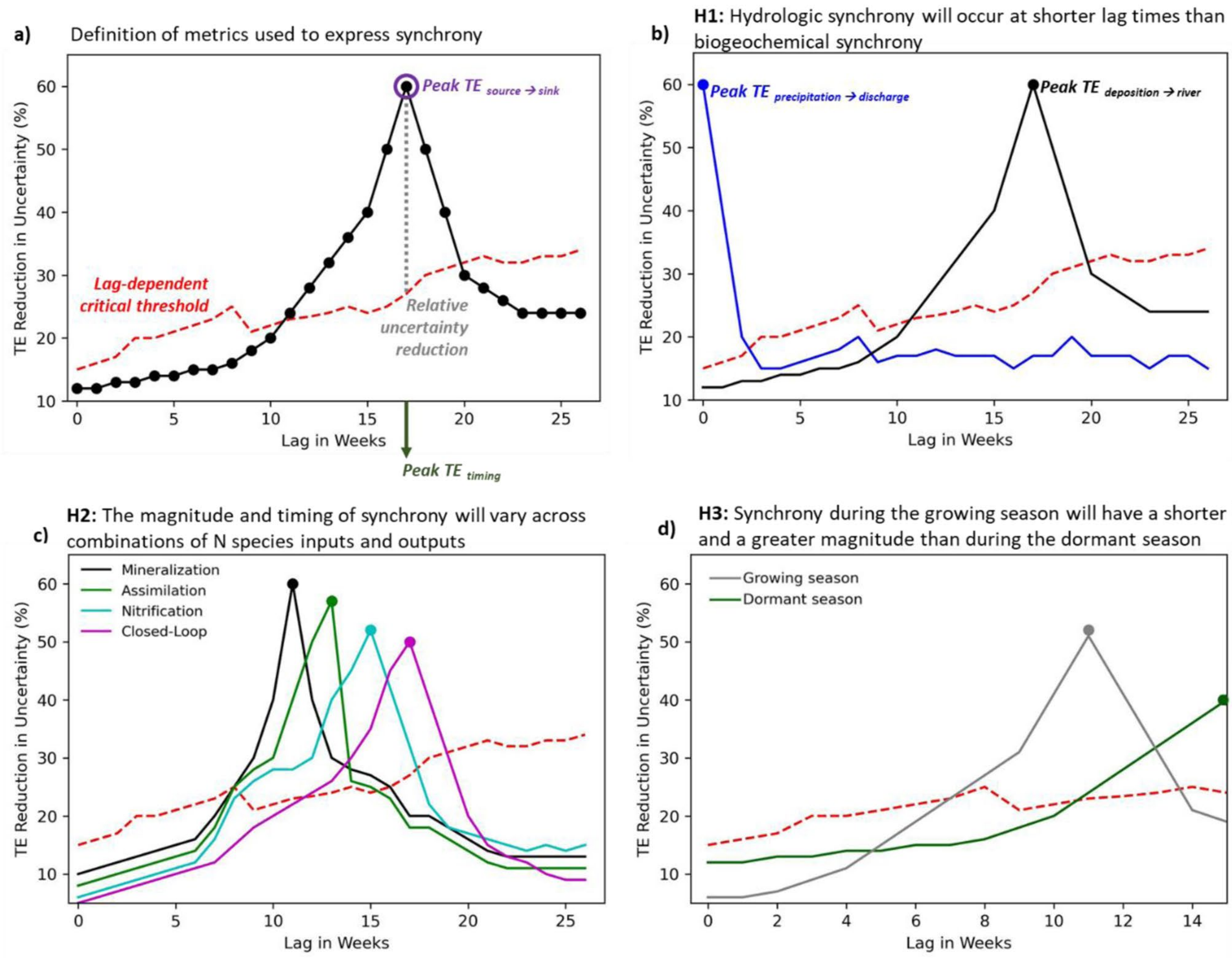

Figure 1. (a) Definition of metrics for transfer entropy (TE) peak relative reduction in uncertainty, timing of peak uncertainty reduction (peak TE), and lag-dependent critical threshold derived from lagged TE values normalized by the Shannon entropy of the "sink" variable. The *y*-axis represents the fraction of uncertainty in the sink (here, river N concentration) explained by the knowledge of past values of the "source," or wet deposition. Higher TE values correspond to a greater reduction in uncertainty of the sink variable. The critical threshold line represents the statistical significance threshold determined based on the 95th percentile distribution of the Monte Carlo analysis (panel a). Panels (b–d) represent conceptual diagrams for predicted TE results for (b) H1, (c) H2, and (d) H3.

spiraling (like-with-like solutes at longer lag times; i.e., mineralization → nitrification → assimilation → mineralization) and advection (like-with-like solutes at lag times overlapping with hydrologic synchrony). Importantly, the information theory algorithm employed cannot differentiate between N transformation occurring in the terrestrial versus riverine component of the watershed box and thus we treat signals of N processing as integrated signals of an entire watershed.

We formed hypotheses (Figure 1) of wet deposition-river N synchrony that considered the transformations wet deposition N may undergo in either the terrestrial and aquatic ecosystems, viewing the watershed as a non-linear filter that moves precipitation from the atmosphere to the stream network (Kirchner, 2009; Kirchner et al., 2001). Given the variable temporal scales that govern hydrologic and biogeochemical connectivity, we first hypothesized that (H1) precipitation and discharge would be synchronized at shorter lag times than synchrony between wet deposition inputs and river outputs across combinations of N species. Second, we hypothesized that (H2) the magnitude and timing of synchrony between wet deposition inputs and river outputs would vary across combinations of N species. Specifically, we predicted that mineralization ($DON_{deposition} \times NH_4{}^+{}_{river}$) and assimilation ($NH_4{}^+{}_{deposition} \times DON_{river}$) would display the strongest synchrony due to the facultatively aerobic conditions required for these transformations over obligatory aerobic conditions required for dissimilatory processes such as nitrification. Lastly, we hypothesized that (H3) the synchrony between wet deposition inputs and watershed outputs during the growing season

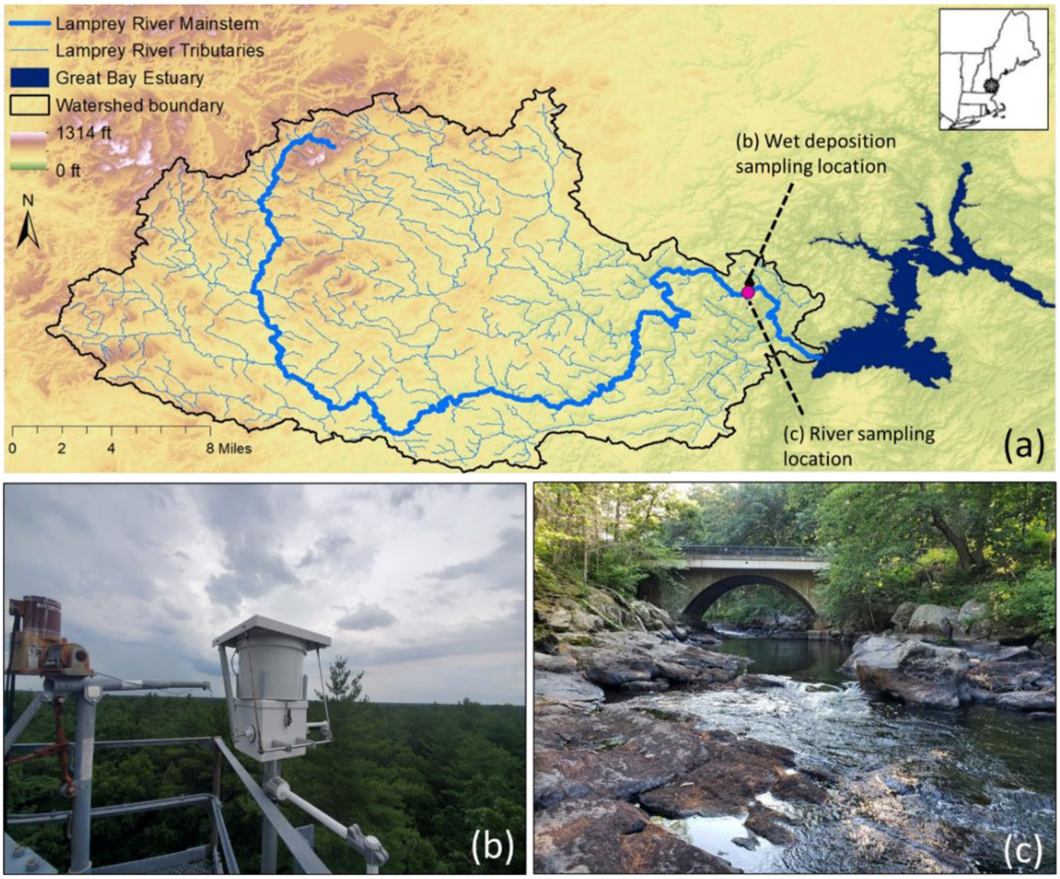

Figure 2. Map of the Lamprey River watershed (a) in southeastern New Hampshire (USA). The wet deposition samples are collected from Thompson Farm wet deposition collector located on top of a 30 m walk-up tower (a) and the river water samples are collected from the mainstem of the Lamprey River (c). Photos were taken in July 2022.

(May–October) would be stronger and at a shorter lag than that during the dormant season (November–April), due to the role of phenomena such as snow accumulation disconnecting deposition inputs to watershed outputs (Franzen et al., 2020). We further predicted that increasing wet deposition loading of N solutes would correspond to increases of riverine N solutes (Brookshire et al., 2007; Templer et al., 2022) at the time lag corresponding to the peak uncertainty reduction. Together with foundational biogeochemical understanding, our analyses can be used to generate hypotheses and conceptual models of ecosystem processes driving atmosphere-river N synchrony.

2. Materials and Methods

2.1. Study Location

We apply information theory to a simplistic watershed budget model approach (e.g., $N_{outputs} = N_{inputs} - N_{storage}$) to derive mechanistic inferences on the fate of N in watersheds. We used 17 years (December 2003–September 2021) of weekly, year-round spatial-temporally paired timeseries of wet deposition and river N concentrations from the Lamprey River Hydrological Observatory (Wymore et al., 2021). The Lamprey River watershed, located in southeastern New Hampshire (USA), drains 554 km^2 of low-elevation terrain before entering the Great Bay Estuary (Figure 2). The watershed is primarily forested (73%), but agriculture (5%), wetlands (10%), and developed areas (7%) are also present (Wymore et al., 2021). During the study period, the mean annual air temperature was 9.2 ± 0.8°C and the site received an average of 127 ± 6 cm of precipitation per year, with 2%–16% falling as snow (Murray et al., 2022).

2.2. Wet Deposition and River Water Sample Collection

Hourly precipitation depth (mm) is measured at the Climate Reference Network (CRN; GHCND: USW00054795; NH Durham 2 SSW) weather station located 22 m from the ACM 301 collector and 295 m from the N-CON

10.1029/2023WR034794

collector. Lamprey River discharge (15-min) was collected from the U.S. Geological Survey (USGS) gaging station 01073500, which is co-located with the surface water chemistry sampling site (Figure 2). Discharge was scaled to watershed area and then assigned a wet deposition sampling interval using the same method as the surface water samples, resulting in a paired weekly total discharge (mm/week) and precipitation depth (mm) timeseries.

Wet deposition data were collected from Thompson Farm (TF; 43.11°N, 70.95°W), located approximately 0.6 km from the surface water collection site (Figure 2). The wet deposition and surface water collection sites are 23 m above sea level (Figure 2), 20 km from the Atlantic Ocean and surrounded by mixed deciduous and coniferous forests and agricultural fields. An Aerochem Metrics (ACM) 301 wet-only precipitation collector located in an open field was used from 2003 to 2008, and an N-CON Systems Company Inc. Atmospheric Deposition Sampler (Model 00–120) located on a 30 m walk-up tower was used from 2009 to 2021 (Liptzin et al., 2013). The open field collector and tower collector are approximately 300 m apart. We conducted year-round event-based sampling through 2008. From 2009 to 2021 samples were collected on a weekly basis. Collection buckets and lids were washed with a <0.1% hydrochloric acid solution (HCl), soaked in deionized water, and rinsed three or more times with deionized (DI) water before deployment. Buckets were changed after 7 days even if no precipitation occurred. Precipitation chemistry is representative of the cumulative conditions during the sampling window. River water grab samples were collected weekly from the mainstem of the Lamprey River (43.10°N, 70.95°W; Figure 2) from 2003 to 2021.

2.3. Wet Chemistry Analyses

Both wet deposition and river samples were analyzed at the University of New Hampshire Water Quality Analysis Laboratory. All samples were filtered through pre-combusted (450°C for 4–6 hr) 0.7 μm Whatman glass-fiber filters (GF/F), stored in acid-washed (10% HCl) HDPE bottles that were rinsed three times with DI water and rinsed three times with filtered sample before filling, and frozen until analysis. Nitrate was measured using a Dionex Ion Chromatograph with suppressed conductivity detection (based on EPA 300.1; detection limit (DL) = 0.004 mg N/L). Analysis of NH_4^+ was done by colorimetric determination using the automated phenate method (based on EPA 350.1) on a Lachat Quickchem AE until 2004, and on a SmartChem, Westco Scientific Instruments automated discrete analyzer from 2004 to 2021 (DL = 0.004 mg N/L). TDN was analyzed on a high-temperature catalytic oxidation Shimadzu TOC-VCSH (Shimadzu Corporation, Kyoto, Japan) with a TNM-1 Total Nitrogen Module until 2014 (DL = 0.07 mg N/L), and on a Shimadzu TOC-LCSH with a TNM-1 (DL = 0.05 mg N/L) since 2014. Laboratory reagent blanks, laboratory duplicates, field duplicates, and certified reference materials were included in each analytical sequence to ensure quality control. Measures of NO_3^- and NH_4^+ represent the atomic portion of N and are reported as NO_3-N and NH_4-N. Data below the DL were assigned ½ the DL. For deposition solutes, less than 2% of TDN, NO_3-N and NH_4-N values were below DL. For riverine solutes all TDN observations were above the DL while 1% and 5.6% of NO_3-N and NH_4-N observations were below the DL, respectively. Concentrations of DON were determined as the difference between DL-corrected total dissolved nitrogen and dissolved inorganic nitrogen (DIN), where DIN is the sum of DL-corrected NO_3^- and NH_4^+. Negative DON values were assigned a zero (see Murray et al., 2022). Forty percent of total deposition DON observations were assigned a zero-value while only 0.1% of river DON observations were assigned a zero.

2.4. Timeseries Pre-Processing

We analyzed information flows for all pair-wise combinations of these N species that correspond to the most dominant and plausible biogeochemical transformations in the N cycle, as well as hydrologic information flows from precipitation to streamflow. A river sample was considered paired with a wet deposition sample if the river sample was collected after the deposition sample deployment date and on or before the next wet deposition sample collection date. We acknowledge that deposition and riverine N samples are collected differently (i.e., cumulative over a week vs. instantaneous concentration, respectively), and thus we assume that the riverine grab sample chemistry is representative of the conditions during the entire wet deposition collection window.

Compared to other standard timeseries analyses, calculation of information-theory metrics requires less pre-processing. However, due to seasonality within the Lamprey River watershed wet deposition and river timeseries (Fazekas et al., 2021; Murray et al., 2022), all data were de-trended by calculating information transfer

10.1029/2023WR034794

on weekly anomalies (($\phi_w = y_w - \bar{y_w}$)) where $\bar{y_w}$ is the long-term average value across the entire timeseries for each week of the year (w), which is subtracted from the observed value (y_w). A weekly anomaly aggregation was chosen because the median duration of each wet deposition sampling window was 6.7 days, and the river samples are collected on a weekly basis.

Calculating information transfer on anomaly timeseries reduces the inherent information transfer resulting from seasonal cycles of precipitation and stream timeseries (Franzen et al., 2020; Ruddell & Kumar, 2009). Removal of seasonal cycles to look at anomalies makes it more likely that significant resulting synchronicities are due to mechanistic connections between the variables. To resolve non-null seasonal differences in biogeochemical information flows resulting from process differences related to snow accumulation and phenology, anomaly data were aggregated into the growing season (May–October) and the dormant season (November–April), corresponding to the distinct phenology experienced in northern temperate forests (Contosta et al., 2017). Information theory algorithms were applied to weekly paired wet deposition and river N concentrations for the full data record (n = 989–1,025), dormant season (n = 488–507) and growing season (n = 501–520). Frequency distribution of anomaly timeseries can be found in the supplemental files (Figure S3 in Supporting Information S1).

2.5. Separating Hydrologic and Biogeochemical (a)synchrony

Like in-stream nutrient spiraling models (Ensign & Doyle, 2006), the transport and transformation of solutes between precipitation and a river is under both hydrological and biogeochemical controls. For the biogeochemical analyses we used concentrations of N (mg N L^{-1}) in wet deposition and the river, over fluxes (mg N L^{-1} $time^{-1}$), because the latter approach would introduce a large source of uncertainty as precipitation amount is highly uncertain at the watershed scale. Nonetheless, quantifying information transfer between the precipitation and discharge timeseries provides a crucial baseline for interpreting information transfer from the biogeochemical analyses. To address the role of hydrology, however, a hydrologically based analysis was also run for precipitation and discharge time series, serving as a null analysis accounting for hydrological synchrony alone. We assume that if the TE_{timing} from the biogeochemical analyses exceeds any significant timescales of hydrologic-process synchrony, then both forcings are acting upon N that has been deposited in the watershed (e.g., Figure 1b). However, if information transfer timescales associated with the hydrologic analysis exceed, or are equal to, the timescale of peak biogeochemical information flow, then we assume that hydrologic processes are the primary driver of the fate of N wet deposition. This comparison facilitates any biogeochemical causal inferences, such as transient storage and subsequent N transformations, by accounting for the underlying role of hydrologic processes, such as advection.

2.6. Information Theory Implementation

From the weekly anomalies for all pair-wise combinations of N species we computed the information transfer from the source variable (wet deposition) to the sink variable (river). The time lags (τ) investigated range from no lag (i.e., 0 weeks) to 26 weeks for the full data range, and 0–13 weeks for the dormant and growing season subsets. This range of lag times ensures that enough data is passed through the information metric calculations for results to be statistically robust but presumes that resolvable information transfer from wet deposition to river occurs on a timescale less than a single calendar year or growing/dormant season.

The computation of $H(X)$, MI, and TE (Equations 1–3) requires obtaining a probability distribution function (pdf) of the source and sink anomaly timeseries. Statistically robust TE calculations should use at least 500–1,000 data points distributed across 10–20 bins, with 11 bins providing adequate robustness and accuracy (Ruddell & Kumar, 2009). Thus, we used a histogram approach of 11 bins to derive the pdf. Zero and non-zero values were separated in the binning process (Chapman, 1986; Gong et al., 2014) so that non-events (i.e., cases where no precipitation fell or an N solute was not detected), are represented in the discretized pdf as a separate "process" from events (Moges, Ruddell, Zhang, Driscoll, Norton, et al., 2022). The binned joint and conditional probability distributions underlying the TE computation (Equation 3) are computed only from existing data, with no gap-filling. That is, transitions in stream solute concentration from one bin of values to another over a time step, conditioned on the bin value of the deposition concentration at a lag, are tallied in the discretized probability computation only if stream chemistry data and the current and previous timestep and deposition chemistry data at the specified lag exist.

Lag-dependent statistical significance of TE values was assessed using a Monte Carlo approach to avoid type 2 error (i.e., false-negative). Experimentally derived TE values were compared to those calculated from 500

10.1029/2023WR034794

incidences in which the portion of the lagged timeseries overlapping (i.e., paired with) the unlagged series was randomly shuffled to remove any existing temporal autocorrelation between the two variables. The 95th percentile score for TE from the randomized samples was used as the "lag-dependent critical value" (akin to a p-value determined at the 0.05 level). As such, TE values exceeding the 95th percentile critical value were considered significant, corresponding to "resolvable" synchrony (Figure 1a).

Information transfer metrics are quantified in bits of information. However, for ease of interpretation, TE is often normalized by the assumed sink variable's entropy (e.g., TE $(X, Y)/H(Y)$) and expressed as a percent reduction in uncertainty. A normalized TE of 0 indicates the two timeseries are completely independent (i.e., knowing everything about one timeseries informs nothing about the other), whereas a normalized TE of 1 indicates that one timeseries is perfectly predictive of the other. We report TE values normalized in this way as relative to the "lag-dependent critical value" by calculating the distance between the normalized TE value and normalized critical value at each lag (Figure 1a). In other words, a normalized TE can be thought of as the relative *percent* reduction in uncertainty (Figure 1a) of river N chemistry based on knowledge of wet deposition N chemistry and conditioned on the river's N chemistry history (Larsen & Harvey, 2017; Moges, Ruddell, Zhang, Driscoll, & Larsen, 2022; Ruddell & Kumar, 2009; Schreiber, 2000). All data were analyzed in Python 3.10.4. and scripts were sourced and modified with permission from Moges, Ruddell, Zhang, Driscoll, and Larsen (2022) and Moges, Ruddell, Zhang, Driscoll, Norton, et al. (2022).

2.7. Concentration Relationships Between Wet Deposition and River N

Information theory results can support mechanistic inferences within hydrologic systems (Franzen et al., 2020; Moges, Ruddell, Zhang, Driscoll, & Larsen, 2022; Tennant et al., 2020). For pair-wise combinations of N species with significant TE and MI results (see supplemental information for MI results), wet deposition values were matched to the corresponding river variables based on the timing of the metric that was associated with the peak reduction in uncertainty (Figure 1). For example, if peak information transfer between wet deposition and river timeseries occurred at 17 weeks (i.e., Figure 1a) the deposition timeseries was shifted to that corresponding river value (i.e., wet deposition at 0-weeks corresponds to river observation at 10 weeks into the future). Each iteration of the shifted deposition and river timeseries were binned into quantiles (5th, 10th, 20th, 30th, 40th, 50th, 60th, 70th, 80th, 90th, 95th) and the median and standard error of the wet deposition and corresponding river data within each bin was calculated. Un-binned relationships between wet deposition and river solutes can be found in the supplemental files (Figure S6 in Supporting Information S1). A logarithmic function was applied to the binned percentile median wet deposition and river values for all shifted timeseries. We represent the goodness of fit of the logarithmic function using the coefficient of determination (R^2). The direction and fit of the logarithmic functions at the timing of peak synchrony was used to evaluate whether our prediction that increasing wet deposition loading of N solutes will correspond to increases of in-river N solutes, as has been observed in other studies (e.g., Brookshire et al., 2007; Templer et al., 2022).

3. Results

3.1. Timeseries Variability

Across the 17-years data record, precipitation depth showed no clear intra-annual variability, ranging from 0 to 292 mm (Figure 3a) and little seasonality (Figure S1 in Supporting Information S1). Variability in mean runoff (i.e., discharge depth (mm)) was orders of magnitude higher than mean precipitation depth and showed some seasonality, with higher mean runoff occurring during the dormant season (Figure 3b). For the biogeochemical analyses, the week-of-year mean values showed differences in magnitude and seasonality between the wet deposition and river timeseries (Figures 3c–3h). Wet deposition DON concentrations ranged from 0 to 1.1 mg N/L, with peak concentrations occurring in the growing season, particularly May and June (Figure 3c). River DON (0–1.01 mg N/L) concentrations were of a similar magnitude to wet deposition DON concentrations and also had greater concentrations during the growing season (Figure 3f). Wet deposition NH_4^+ concentrations ranged from 0.002 to 3.7 mg N/L (Figure 3e), while river NH_4^+ concentrations were much lower, ranging from 0.002 to 0.2 mg N/L (Figure 3f), but both timeseries showed consistent variability throughout the year. Wet deposition NO_3^- concentrations were highly variable throughout the year, ranging from 0.003 to 2 mg N/L (Figure 3g); river NO_3^- concentrations ranged from 0.003 to 0.6 mg N/L and showed consistently high concentrations during the dormant season (Figure 3h).

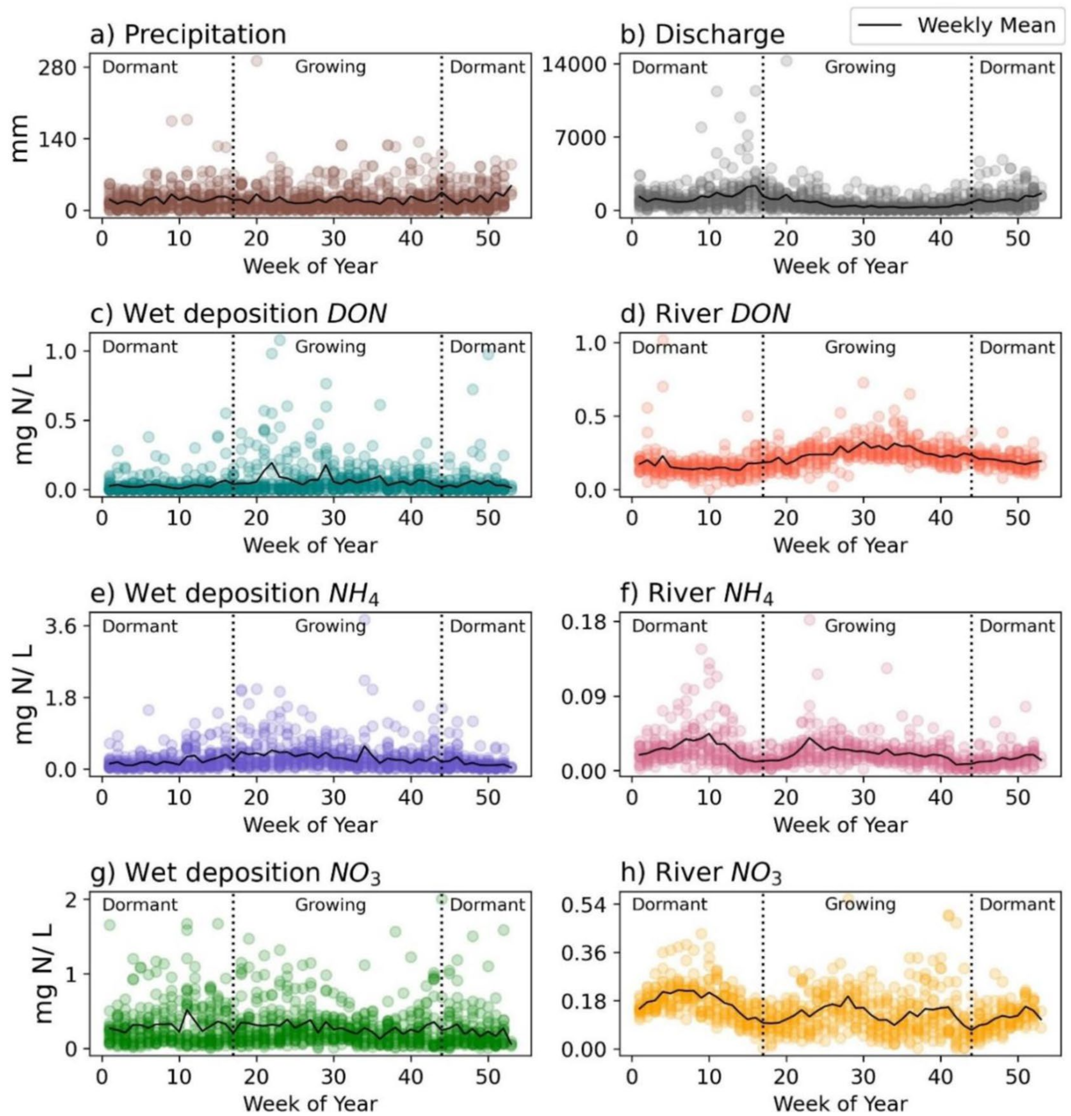

Figure 3. Week of year timeseries of (a) precipitation depth, (b) discharge depth, (c) wet deposition DON concentration, (d) river DON concentration, (e) wet deposition NH_4^+ concentration, (f) river NH_4^+ concentration, (g) wet deposition NO_3^- concentration, and (h) river NO_3^- concentration. The black line represents the week-of-year mean for all 17-years of data. Scatter plots of the week of year anomalies can be found in Figure S2 of the Supporting Information S1.

Shannon entropy [$H(Y)$], or the measure of information content (equivalent to uncertainty) in the full data records for river DON, NO_3^-, and NH_4^+ ranged from 2 to 2.4 bits (Table 1). The lowest information content occurred in river DON concentrations and the highest information was found for river NO_3^- concentrations (Table 1). When data were aggregated seasonally, information content of river timeseries increased. Shannon entropy of river DON and NH_4^+ timeseries was higher in the growing season as compared to the dormant season (Table 1) while $H(Y)$ for river NO_3^- was highest during the dormant season at 2.8 bits (Table 1). Discharge $H(Y)$ was less than the $H(Y)$ of biogeochemical analytes, at 1.6, 1.9, and 2.2 bits for the full record, dormant and growing seasons, respectively (Table 1).

3.2. Hydrologic Analysis

Consistent with H1, which predicted that precipitation and discharge would be synchronized at shorter lag times than wet deposition inputs and outputs across combinations of N species, we found that river discharge uncertainty was most reduced by information provided to discharge from weekly precipitation on short time lags

10.1029/2023WR034794

Table 1
Ranges of Significant Transfer Entropy (TE) Values for the Full Data Record, Dormant Season, and Growing Season for Each Wet Deposition and River Paired Timeseries

	Full data record (n = 989–1,025)			Dormant season: November–April (n = 488–507)			Growing season: May–October (n = 501–520)		
Wet deposition × river	$H(Y)$, bits	Lags, week	TE relative uncertainty reduction	$H(Y)$, bits	Lags, week	TE relative uncertainty reduction	$H(Y)$, bits	Lags, week	TE relative uncertainty reduction
P × Q	1.6	0–5	0.2%–5.2%	1.9	0, 2	0.6%–3.1%	2.2	0	1.7%
$NH_4^+ \times NO_3^-$	2.4	17	0.9%	2.8	–	–	2.6	–	–
DON × NH_4^+	2.2	0–20	0.1%–1.2%	2.4	–	–	2.6	0–8	0.7%–6.1%
DON × NO_3^-	2.4	0–24	0.1%–2.6%	2.8	–	–	2.6	–	–
NH_4^+ × DON	2.0	12	0.2%	2.0	0	0.1%	2.5	–	–
NO_3^- × DON	2.0	17	0.5%	2.0	–	–	2.5	–	–
DON × DON	2.0	12–24	0.1%–1.7%	2.0	–	–	2.5	–	–
$NH_4^+ \times NH_4^+$	2.2	–	–	2.4	–	–	2.6	0–8	1%–5.2%
$NO_3^- \times NO_3^-$	2.4	–	–	2.8	9	0.6%	2.6	0, 10	0.3%–1%

Note. Normalized TE values are presented as the relative percent (%) reduction in uncertainty from the total information held within the sink variable [$H(Y)$, in bits] at a given lag (in weeks). Non-significant results are noted with "–."

(<1 week), combined with antecedent conditions of discharge. Persistence of information transfer from precipitation to discharge continued for three consecutive lag times (i.e., 0, 1, and 2 weeks), with significant TE also occurring at 5 weeks lag (Table 1). Seasonal hydrologic information transfer was greater during the dormant season—significant at 0- and 2-weeks lag—while information transfer during the growing season did not persist beyond 0 weeks lag (Table 1).

Hydrologic TE results are used to interpret whether information transfer from biogeochemical analyses is driven by hydrologic and/or biogeochemical processes (see Section 2.5). Consistent with H1, the magnitude and timing of uncertainty reductions for the hydrologic analysis displayed significant information transfer at lag times shorter than peak TE_{timing} for most biogeochemical analyses (Figure 4). However, peak TE_{timing} between $DON_{deposition} \times NH_4^+{}_{river}$ for the full record and growing season, as well as for $NH_4^+{}_{deposition} \times DON_{river}$ in the dormant season, overlapped with timescales of hydrologic TE_{timing} (Figure 4).

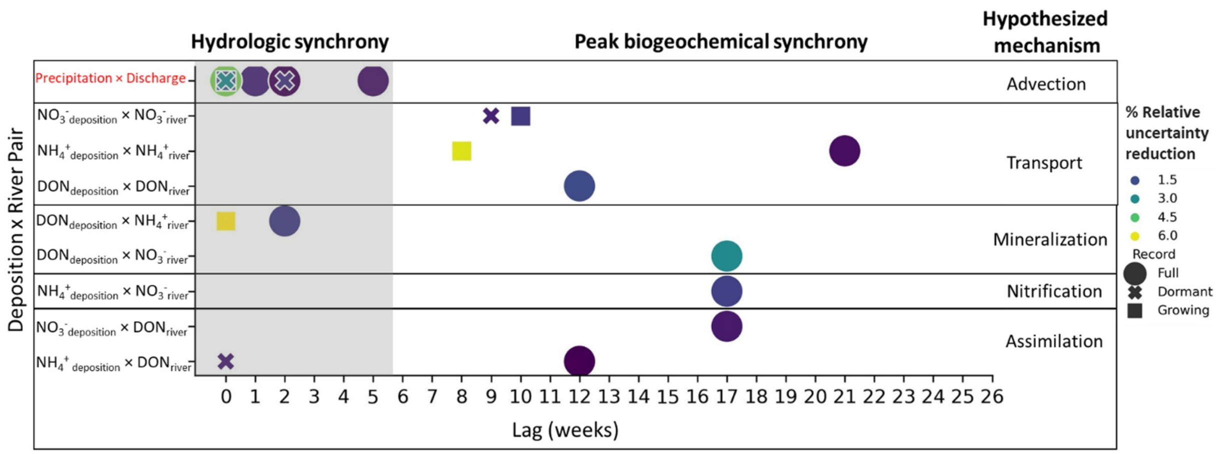

Figure 4. Hydrologic synchrony expressed as the relative normalized percent (%) uncertainty reduction (i.e., TE $(X, Y)/H(Y)*100$—the significance threshold) scaled from blue (low) to yellow (high) for the hydrologic pair ($P \times Q$) for *all* lags with significant $TE_{deposition \rightarrow river}$ (e.g., TE values above the critical threshold value). The gray shaded area indicates the persistence of significant synchrony for the hydrologic analysis. Biogeochemical synchrony is shown *only* for peak TE_{timing} and is categorized by hypothesized processes (i.e., $NH_4^+{}_{deposition} \times NO_3^-{}_{river}$ indicates nitrification) for the full record (circle), dormant (x) and growing (square) seasons.

10.1029/2023WR034794

3.3. Biogeochemical Analyses

Results supported H2, which predicted that the magnitude and timing of synchrony between wet deposition inputs and river outputs would vary across combinations of N species, specifically, that mineralization ($DON_{deposition} \times NH_4{}^+{}_{river}$) and assimilation ($NH_4{}^+{}_{deposition} \times DON_{river}$) would display the strongest synchrony. We found that each wet deposition-river N pairing displayed varying strengths and timing of significant TE. Significant TE was resolved for pair-wise combinations that were indicative of transformations from $NH_4{}^+{}_{deposition} \times NO_3{}^-{}_{river}$ (i.e., nitrification), inorganic N wet deposition and organic N river (i.e., mineralization), organic N wet deposition to inorganic N river (i.e., assimilation) as well as solute to solute (i.e., advection at short lags or closed-loop spiraling at long lags). While the normalized uncertainty reduction (i.e., TE $(X,Y)/H(Y)*100$) ranged from 30% to 80% (Figure S4 in Supporting Information S1), the lag-dependent critical threshold values resolved from re-shuffling of the timeseries were also high (see supplemental files), resulting in relative uncertainty reductions (i.e., the distance between the normalized TE value and normalized critical value at each lag) ranging from <1% to 6% (Table 1). The biogeochemical analyses with the highest amount of relative uncertainty reductions for each data segmentation scheme were $DON_{deposition} \times NO_3{}^-{}_{river}$ at 3% for the full record, $NO_3{}^-{}_{deposition} \times NO_3{}^-{}_{river}$ at 0.6% in the dormant season, and $DON_{deposition} \times NH_4{}^+{}_{river}$ at 6% in the growing season (Table 1). Across all pairwise combinations, river DON concentrations consistently received the most information from all three wet deposition solutes compared to river inorganic N concentrations. Wet deposition DON and $NH_4{}^+$ contributed the information to, or reduced the uncertainty for, all three river N solutes.

For the full record analyses, the timing of biogeochemical synchrony ranged from 12 to 21 weeks (Table 1) depending on the solute pair, indicating a gradient of watershed reaction rates and retention times. At 12 weeks lag, TE between $NH_4{}^+{}_{deposition} \times DON_{river}$ and $DON_{deposition} \times DON_{river}$ peaked (Figure 4). In contrast, peak TE between $NO_3{}^-{}_{deposition} \times DON_{river}$, $NH_4{}^+{}_{deposition} \times NO_3{}^-{}_{river}$ and $DON_{deposition} \times NO_3{}^-{}_{river}$ occurred at 17 weeks lag (Figure 4), and peak TE between $NH_4{}^+{}_{deposition} \times NH_4{}^+{}_{river}$ occurred at 21 weeks lag (Figure 4). Contrary to H3, in which we predicted that the synchrony between wet deposition inputs and watershed outputs during the growing season would be stronger and at a shorter lag than that during the dormant season, dormant and growing seasonal analyses did not produce different results. The magnitude of relative uncertainty reductions was similar for the seasonal analyses and the full record; however, fewer wet deposition-river solute pairs were significant for the seasonal analyses (Table 1; Figure 4). When data were aggregated seasonally, TE was significant only for inorganic N pairs corresponding to closed-loop spiraling (Table 1), with peak uncertainty reductions occurring at 8–10 weeks lag (Figure 4).

The relationship between wet deposition N and river N timeseries lagged at peak TE_{timing} displayed both increasing and decreasing non-linear relationships with respect to median concentrations within each percentile bin (Figure 5). This finding contrasts with our initial prediction that wet deposition loading of N solutes will consistently correspond to increases of river N solutes. The relationship between precipitation depth and discharge depth at no lag displayed a positive, increasing relationship ($R^2 = 0.90$) with some asymptotic behavior at high precipitation and discharge depths (Figure 5a). Similarly, DON concentrations in river water increased with median concentrations of wet deposition DON ($R^2 = 0.80$) and $NH_4{}^+$ ($R^2 = 0.89$) when examining the concentration relationship at 12-weeks lag (Figures 5b and 5c). In contrast, concentrations of median riverine $NO_3{}^-$ declined with increasing wet deposition DON ($R^2 = 0.23$) and $NH_4{}^+$ ($R^2 = 0.85$) concentrations when examining the concentration relationship at 17-weeks lag (Figures 5d and 5e). The response of $NH_4{}^+$ river concentrations lagged 21 weeks to $NH_4{}^+$ deposition concentrations showed a similar negative relationship ($R^2 = 0.41$) with asymptotic behavior at high deposition concentrations (Figure 5f).

4. Discussion

This study used information theory to detect synchrony between timeseries of wet deposition N inputs and river N outputs. We view synchrony as the embodiment of not only linear processes but also complex non-linear interactions that lead to high spatiotemporal coherence and consistent lagged behavior through time (Seybold, Fork, et al., 2022). Here, synchrony is quantified as a significant amount of information transfer between wet deposition and river N timeseries resulting in a reduction in uncertainty of the sink variable. Differences between hydrologic (i.e., *P-Q*) and biogeochemical (i.e., N-solute pairs) transfer entropy indicate that N dissolved in precipitation is subject to biogeochemical transformations in addition to advection processes. Pair-wise combinations of wet deposition and river N that follow likely biogeochemical transformations in the N cycle showed varying degrees

10.1029/2023WR034794

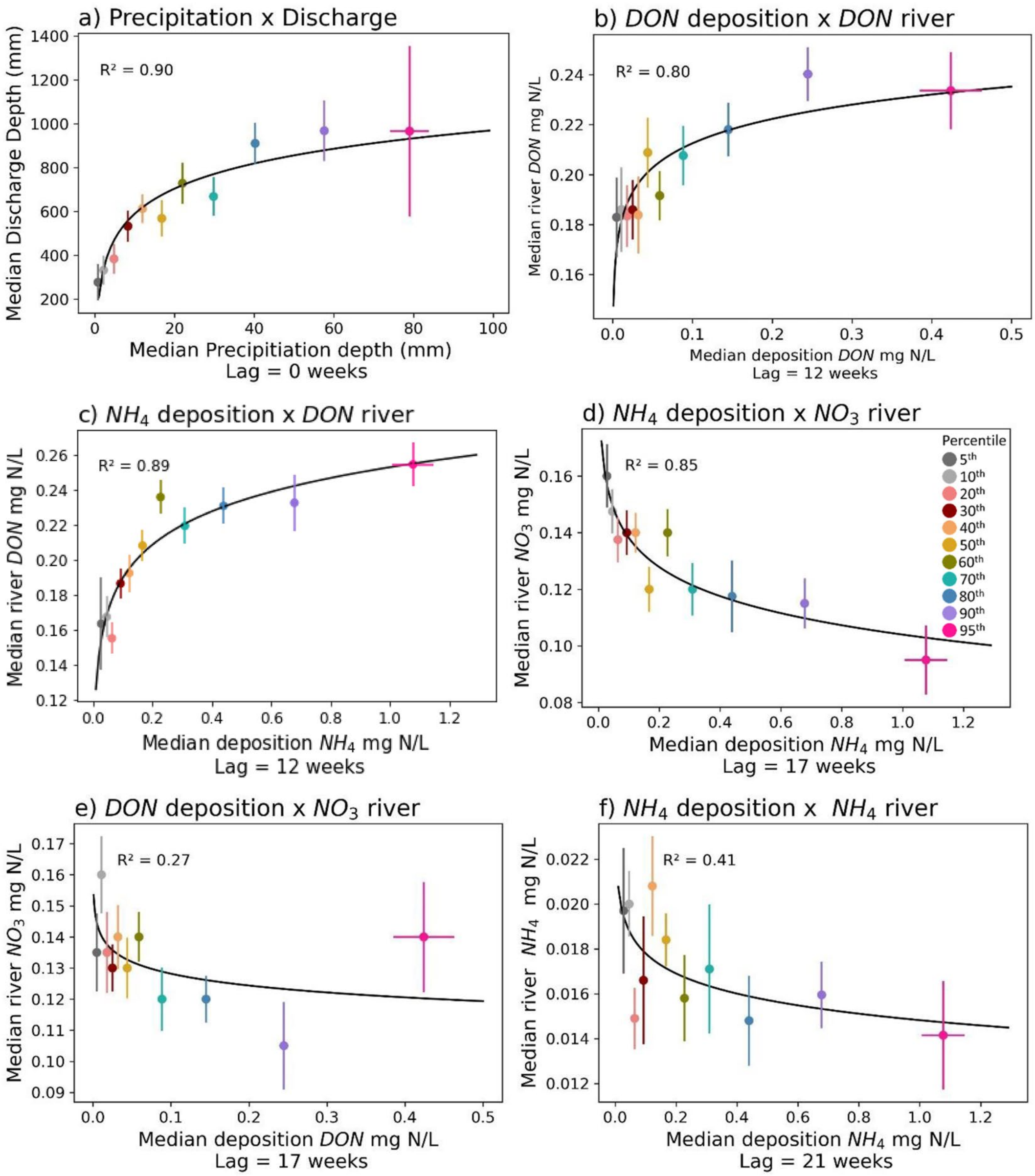

Figure 5. Logistic regressions between median (±1 SE in the *x* and *y* direction) wet deposition and river variables within each wet deposition percentile bin shifted to the lag corresponding with peak TE_{timing} for (a) precipitation depth × river discharge depth at 0 lag; (b) $DON_{deposition}$ lagged 12 weeks × DON_{river}; (c) $NH_4^+{}_{deposition}$ lagged 12 weeks × DON_{river}; (d) $NH_4^+{}_{deposition}$ lagged 17 weeks × $NO_3^-{}_{river}$; (e) $DON_{deposition}$ lagged 17 weeks × $NO_3^-{}_{river}$; and (f) $NH_4^+{}_{deposition}$ lagged 21 weeks × $NH_4^+{}_{river}$. The solid black line corresponds to the best fit logarithmic function with the R^2 value provided. These plots display the directionality of the response of the sink variable (river timeseries) to the lagged source variable (wet deposition timeseries) at peak TE_{timing}.

of lag times, synchrony, and input-output concentration relationships (Figures 4 and 5), likely due to the gradient of environmental conditions required for each reaction to occur. Information theoretic algorithms facilitated empirically derived mechanistic inferences on the hydro-biogeochemical processes that contribute to the fate of N wet deposition entering the Lamprey River watershed; for example, N assimilation is a positive lagged function of increasing N wet deposition (Figure 5). These results provide insights into probable biogeochemical N pathways occurring within our study watershed. We conclude that although wet deposition N is not the main driver of river N, it does contribute a significant amount of information that is resolvable at realistic time lags, which provides insights into identifiable biogeochemical transformations occurring within the landscape.

10.1029/2023WR034794

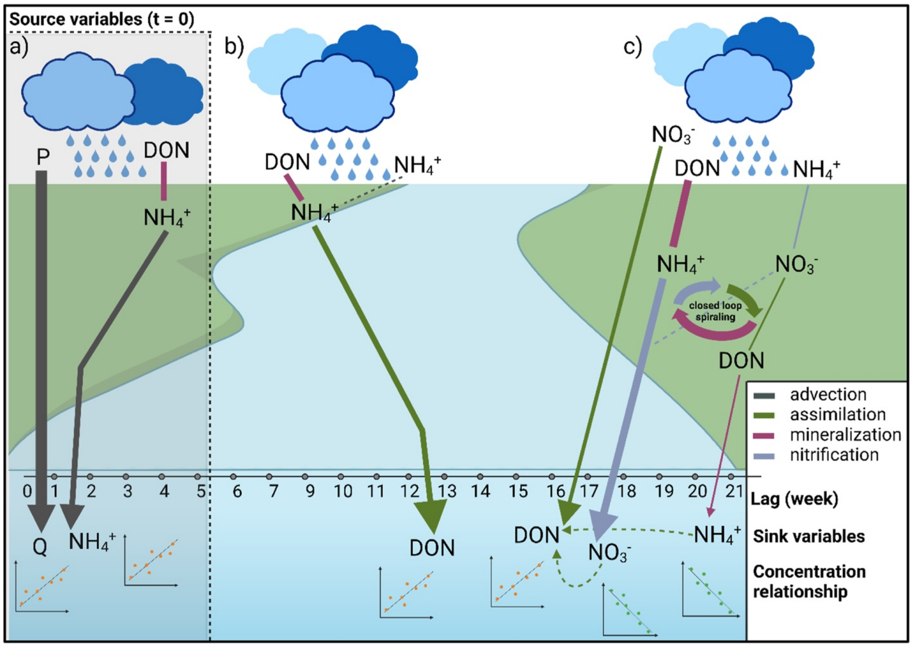

Figure 6. Conceptual model of the hypothesized fate of N deposition upon entering the Lamprey River watershed for (a) hydrologic synchrony from 0 to 5 weeks lag, and biogeochemical synchrony at (b) 12-weeks, and (c)17- weeks and 21-weeks. The size of the arrow scales with the magnitude of relative normalized percent uncertainty reductions (Figure 4) informed by the maximum information transfer and associated lag times for the full data record. The colors reflect the hypothesized hydro-biogeochemical mechanisms that may explain the observed uncertainty reductions. The bottom row of scatter plots shows the simplified relationship between source variables on the *x*-axis (e.g., precipitation depth and wet deposition N concentration) and sink variables on the *y*-axis (discharge depth and river N concentrations) as resolved from shifting the timeseries at peak TE timing and binning into percentiles as seen in Figure 5.

Though significant, wet deposition N does not reduce uncertainty in river N by more than 10% points relative to the significance threshold, indicating that there are other factors working in parallel with wet deposition to control concentrations of riverine N. However, relative TE uncertainty reductions less than 10% are within the range of those reported elsewhere, such as from peatland methane evasion (Sturtevant et al., 2016) and stream metabolism (Larsen & Harvey, 2017). The high lag-dependent critical threshold value is attributed to data record constraints and the inherent noise associated with environmental timeseries where there are many interacting processes that can reduce the likelihood of capturing synchrony with a single source variable (Goodwell et al., 2020). This interpretation is consistent with our contemporary understanding of the links between wet deposition inputs and other vectors of solute generation within watersheds (Likens & Bormann, 1974a, 1974b). For example, other sources of information within the watershed box including throughfall, evapotranspiration, variability of antecedent moisture conditions, precipitation rates, heterogenous soil hydraulic conductivity, soil properties (e.g., wetland histosols) and legacies of in-watershed non-point sources such as agriculture can influence the movement of water and N in a watershed (Baron et al., 2013; Bastviken et al., 2006; Bernal et al., 2012; Jenkinson et al., 1985; Lovett et al., 2000; Whitehead et al., 2009; Wu et al., 2021). Such relationships modify the potential information transfer from wet deposition to river N timeseries, creating variable lags that may occur on timescales longer than those detectable using the maximum lag time considered here.

4.1. Conceptual Model of Watershed N Cycling

Peak transfer entropy results from the full data record (Figure 4) were used to create a mechanistically informed and empirically derived conceptual model of time-scaled wet deposition-river N synchrony (Figure 6). Recognizing there are multiple hydrologic and biogeochemical mechanisms to explain the observed uncertainty reductions described herein, we frame the conceptual model as potential hypotheses. Information theory has yet to be applied to biogeochemical timeseries to make causal inferences, thus we exercise caution when interpreting results by using moments of resolvable synchrony as an opportunity to generate hypotheses of when and

10.1029/2023WR034794

to what magnitude wet deposition nitrogen inputs influence river nitrogen outputs. We base our inferences on the timing of synchrony observed at peak TE_{timing} because this represents the lag at which both hydrologic (i.e., advection) and/or biogeochemical (i.e., N transformation occurring within the watershed) processes that most likely induce the greatest influence on river chemistry. In constructing this conceptual model, we assumed the wet deposition and river chemistry sample locations were representative of the entire catchment due to limited elevation change in the watershed, and because the Lamprey River sampling location was positioned near the river outlet (Figure 2). We did not consider constant leak rates from slow-turnover N pools despite changes in wet deposition inputs (Brookshire et al., 2007). Finally, because our analyses are constrained to paired timeseries that only capture the inputs and outputs of water and N to the Lamprey River watershed, our results from the information theory algorithm can be considered agnostic as to where the potential transformations are occurring (i.e., terrestrial vs. river system).

4.1.1. Hydrologic Synchrony Inferences

The degree of hydrologic synchrony in a watershed is governed in part by the response time of discharge to a precipitation event. We show that conditional discharge uncertainty was most reduced by information provided from precipitation at lag times of less than 1 week (Figures 4 and 6). Persistence of significant information transfer indicates that precipitation continues to contribute information for up to 5 weeks following a precipitation event. This range of significant lag times is also within the range of the 6-weeks average residence time of the shallow groundwater reservoir that is the primary source of baseflow for the headwaters of the Lamprey River (Frades, 2008; Zuidema, 2011).

We found that peak synchrony between weekly precipitation and discharge depth occurring at the minimum lag time considered (i.e., 0-weeks) is consistent with other studies that used TE in sensitivity analyses to show that discharge was sensitive to quick flow generation mechanisms (Moges, Ruddell, Zhang, Driscoll, & Larsen, 2022, Moges, Ruddell, Zhang, Driscoll, Norton, et al., 2022). Synchrony between daily precipitation and discharge values from watersheds across the U.S. ranged from 10% to 60% normalized uncertainty reduction resolved from the transfer entropy algorithm (Moges, Ruddell, Zhang, Driscoll, & Larsen, 2022), which captures the range of normalized uncertainty reduction resolved in this study for weekly precipitation and discharge (20%–40%; Figure S4 in Supporting Information S1). We attributed the positive relationship observed between precipitation depth and discharge depth lagged at the timing of peak synchrony (Figure 5) to be a function of surface flow runoff or advection processes (Figure 6) that occur within 1 week. Notably this relationship was consistent across all significant non-peak lags. While the quantification of specific runoff mechanisms for this watershed is outside the scope of this study, the dominant runoff mechanisms in southeastern New Hampshire are more sensitive to pre-event water storage rather than precipitation intensity (Wu et al., 2021).

Solute pairs with peak TE_{timing} similar to hydrologic synchrony timescales may reflect biogeochemical processes occurring during advection because N transformation timescales are shorter than advection timescales. For example, peak synchrony between $DON_{deposition} \times NH_4^+{}_{river}$ overlapped with timescales of hydrologic synchrony at 2-weeks lag (Figure 6), potentially indicating that either some proportion of DON in precipitation is rapidly mineralized enroute to the stream during advection or is reflective of the flush of water and associated solutes following a precipitation event from short-term storage zones.

4.1.2. Biogeochemical Synchrony Inferences

Solute pairs displaying peak synchrony at timescales longer than hydrologic synchrony may reflect timescales of biogeochemical processing of N in either terrestrial or riverine transient storage zones throughout the entire catchment. This may occur when there is biotic N uptake (Figures 6b and 6c) or when transformations occur preferentially for reservoirs of water that are physically detained within the watershed, either in transient storage pockets (e.g., in wetlands), through sorption to soils (Triska et al., 1994), or along flow paths that are longer than the mean flow path. Although biogeochemical transformations, like rapid mineralization, may occur during advection, as may be the case for $DON_{deposition}$ x $NH_4^+{}_{river}$ (Figure 6a), solute pairs displaying synchrony at longer timescales (Figures 6b and 6c) would only be resolvable from ions dissolved in the fraction of water that has passed through transient storage zones permitting the additional reaction time required for these transformations.

Like-with-like solutes displaying synchrony at longer lag times than precipitation-discharge synchrony must experience retention, uptake, and potentially closed-loop nutrient spiraling (Figure 6c) to not have peak lag times coincide with hydrologic transport timescales. For example, two alternate hypotheses or pathways may

10.1029/2023WR034794

explain the information flows and nature of peak TE timing relationship between $NH_4^+{}_{deposition}$ × $NH_4^+{}_{river}$ with peak synchrony at 21-weeks. First, the 21-weeks lag time could be sufficient for wet depositional NH_4^+ to undergo assimilation, mineralization, and subsequent advection (Figure 6c). Alternatively, the synchrony between $NH_4^+{}_{deposition}$ × $NH_4^+{}_{river}$ could be driven by advection only; however, the long lag time is well outside the lag times resolved for hydrologic synchrony which may discount the potential for advection as the dominant synchrony mechanism for this solute pair (Figure 4). These alternative hypotheses may in fact be occurring at non-peak lag times, as the concentration relationships shown in Figure 5 can vary when examining logistic regression relationships at significant non-peak lag times. The MI results show shorter lags that are more consistent with hydrologic synchrony than the TE results (Table S1; Figure S5 in Supporting Information S1), likely because the peak lag times resolved for MI do not condition information flow on antecedent river conditions and thus may underestimate the role of river antecedent conditions on driving the timing of synchrony between wet deposition N and river N. The results presented herein are reflective of the timing of an entire watershed signal of hydro-biogeochemical processes and do not differentiate the specific watershed box compartments in which such transformations or transport occur. Future studies could leverage paired terrestrial timeseries, such as soil N concentrations, to distinguish the extent to which wet deposition N inputs are transformed within the terrestrial or aquatic system.

The positive relationship between $DON_{deposition}$ × DON_{river} concentrations lagged at 12-weeks (Figure 5) also supports the inference of closed-loop spiraling. Additions of DON via wet deposition correspond to an increase of in-river DON concentration when lagged at peak TE_{timing}, indicating that the mineralization and subsequent assimilation of N is occurring (Figure 6b). Alternatively, if absorption of wet depositional DON were occurring, a negative relationship between inputs and outputs would be expected (Figure 5). However, even at non-peak significant lag times, the relationship was positive. This inference of closed-loop spiraling is supported by the assimilation signal between $NH_4^+{}_{deposition}$ × DON_{river} concentrations (also lagged at 12-weeks) showing a positive relationship, in which inputs of NH_4^+ magnify assimilation processes. The positive concentration relationship between inorganic N wet deposition and organic N river concentrations is supported by other studies examining the relationship between these pools of N at an annual scale (e.g., Brookshire et al., 2007; Templer et al., 2022).

There are potentially competing processes reflected within the information flows resolved in this study. For example, the negative relationship between $NH_4^+{}_{deposition}$ × $NO_3^-{}_{river}$ and $DON_{deposition}$ × $NO_3^-{}_{river}$ (Figure 5) may be explained by competition between heterotrophic and nitrifying bacteria where increases in labile carbon favor heterotrophic assimilation of NH_4^+ over the conversion of NH_4^+ to NO_3^- by nitrifiers (Strauss & Lamberti, 2002). A slowing of nitrification and NO_3^- production may be tied to the increase in assimilation captured at 12-weeks lag (Figure 6), further accelerating uptake of NO_3^- by organisms. Relative to nitrate, NH_4^+ can be rapidly transformed to other forms of N in upland soils, riparian zones, and streams (Causse et al., 2015; Peterson et al., 2001). Increases in DON wet deposition concentrations corresponding to decreases in NO_3^- river concentrations at 17-weeks lag (Figure 5) may alternatively be indicative of losses of NO_3^- via denitrification. Conversion of NO_3^- to N_2 requires anoxic conditions as well as an energy source, which can be provided by DON (Quick et al., 2019; Strauss & Lamberti, 2000; Wymore et al., 2015). While it is well established that allochthonous DOM is an important input of energy to rivers (Vannote et al., 1980) and could promote metabolic pathways for N within the Lamprey River (Herreid et al., 2021), this system is not carbon limited to the extent that DOM deposition would have such a measurable impact on denitrification. Nonetheless, the role of wet deposition DON and DOC to terrestrial and surface water chemistry remains relatively unexplored due to the lack of monitoring for wet deposition organic matter (Cornell, 2011; Liptzin et al., 2022).

We propose these mechanistic inferences as potential hypotheses requiring further experimental vetting. Peak lag times of transfer entropy may be informative for watershed-scale N transit time and may help researchers with experimental design such as tracer experiments. For example, peak lag times coalescing around similar values for multiple solute reactions can be thought of as the "average" or "emergent" (across all years) pattern of how long it takes N and water to be retained and travel through the entire watershed. While the peak biogeochemical lag times are indeed orders of magnitude longer than reaction rates of N transformation (e.g., Li et al., 2020), reaction rates do not account for the time it may take ions to be transported to the river nor for the time for an entire watershed nitrification signal to be manifested in a receiving water body. Peak biogeochemical synchrony between wet deposition-river N coalescing around 12 to 17-weeks lags may reflect bottlenecks of either transformations or transportation to the river. The N biogeochemical reactions resolved at 12 weeks were generally simpler (e.g., fewer transformations or bottlenecks) compared to those at 17 weeks. While the exact water residence time and

N retention time of the Lamprey River watershed is unknown, the watershed does have significant wetlands in the headwaters (Wymore et al., 2021) which could retain water and N for longer periods than can be simulated experimentally.

4.1.3. Seasonal (a)synchrony

The motivation for aggregating analyses by growing and dormant season was to identify the role of phenology in wet deposition-river biogeochemical synchrony. For example, hydrologic and biogeochemical synchrony was less resolvable during the dormant season (Figure 4), likely due to the presence of snow accumulation and frozen soils which can disrupt *P*-*Q* connectivity (Franzen et al., 2020; Tennant et al., 2020). The prevalence of dormant vegetation, snow, and frequent soil freeze-thaw events (Durán et al., 2016; Groffman et al., 2001) may have impacted resolvable N synchrony. We found significant but low-level information flow from wet deposition DON to riverine NH_4^+ at instantaneous to intermediate timescales during the growing season (Figure 4). Synchrony between DON wet deposition and NH_4^+ river during the growing season suggests that mineralization is more prominent in this season due to favorable environmental conditions for plants or microbes like warmer soil temperatures or the presence/absence of co-limiting elements like carbon and oxygen which could facilitate faster rates of mineralization (Craine et al., 2018; Groffman et al., 2018). Differences between information transfer from the full record and seasonal aggregations may be an artifact of the shorter record length and lag times considered, despite the increase of inherent information content (e.g., Shannon entropy; $H(X)$) in the seasonally aggregated timeseries (Table 1). The shorter length of timeseries increases the significance threshold, causing detection of synchrony more difficult to resolve. While our results showed no detectable differences between timing of peak information transfer when assessed seasonally, it is possible that with a longer paired data set, the growing season timeseries could display longer lag times than the dormant season because in the growing season terrestrial vegetation has a higher demand for water and N.

4.2. Implications of Temporal Stationarity

Variability in the length of the dormant and growing season was assumed constant across the 17-years record. Furthermore, the peak lag times resolved from the transfer entropy algorithm are not specific to calendar year and represent the lag time at which deposition and river N timeseries are the most synchronized across all weeks of the years in the 17-years data record. Given the expansion of the vernal window in the northern hemisphere due to warming winters (Contosta et al., 2017; Creed et al., 2015), as well as increased rain-on-snow events across the U.S. (Seybold, Dwivedi, et al., 2022), customizing annual seasonal identification may result in further understanding of how seasonality influences wet deposition-river N (a)synchrony. For example, the stoichiometric ratio of NO_3:NH_4 is on average 4 times more enriched in NO_3^- when precipitation falls as snow in the winter months (Murray et al., 2022), due to precipitation nucleating processes. Future studies could aggregate dormant and growing seasons by an indicator variable such as leaf-out date or air temperature, which would allow for the seasonal signal to reflect changes in phenology and whether phenological variability drives currently synchronous phases to become a-synchronous (Seybold, Fork, et al., 2022).

Importantly, our application of TE to long-term wet deposition-river timeseries assumed temporal stationarity across the data record, despite regional trends of declining wet deposition inorganic N and increases in DON (Murray et al., 2022). TE calculations are run on weekly anomalies, which destroys temporal variability, thus it is likely that signals between deposition and river N would be stronger were we able to account for long-term trends. For example, the mineralization signal from wet deposition DON to river NH_4^+ could become more evident over time given increases in DON deposition concentrations. We also show that river DON concentrations had the most frequent evidence of uncertainty reductions from wet deposition solutes, suggesting that the response of DON, and by extension DOC, is sensitive to wet deposition chemistry. This inference is supported by evidence of surface water browning associated with the ionic load of precipitation (Monteith et al., 2023).

4.3. Using Information Theory to Quantify Watershed-Scale (a)synchrony

Information theory-driven inferences can be helpful for identifying the role of a source variable, such as wet deposition N loading, to ecosystem-scale processes. For example, we find that the magnitude of resolvable synchrony between wet deposition-river N timeseries is low, suggesting that other sources of N loading to the Lamprey River watershed (e.g., wastewater treatment plants, septic systems, wetlands) may also be important targets for mitigation efforts. The magnitude of relative uncertainty reduction imparted by the deposition N timeseries onto the river N timeseries may be greater if we had the ability to leverage a stream chemistry data set collected at the same temporal resolution as the "sink" data. For example, Tennant et al. (2020) found that compounding precipitation data over different timescales (days, weeks, months) reduced variable amounts of uncertainty in stream discharge over select lags, reflecting the inherent timescales of different hydrological phenomena. Notably, snowmelt processes were chiefly detectable from longer-term aggregated precipitation data (e.g., weekly to monthly totals), reflecting the long timescales of snowpack storage. In our data set, weekly aggregated deposition data may provide insufficient resolution to detect timescales of event-based phenomena with low uncertainty but would enable inference of longer-term processes involving watershed detention and storage and impacts of cumulative supply on microbial dynamics. Considering the challenges with creating an appropriately paired sampling regimes over a nearly 20-years data record, this is a reasonable assumption. A future study with a sufficient data record could explore how pairing deposition timeseries with event river samples differs from weekly grab samples. A more integrated metric of river chemistry could be obtained using high-frequency sensors, for example, by taking the average of 15-min measurements over the deposition collection timeframe.

Our results provide evidence that many hydro-biogeochemical interactions are characterized by non-linear, lagged responses (Blöschl & Sivapalan, 1995; Sivapalan et al., 2002). The development of causal inference methods, over correlative methods, is growing in the field of environmental data science largely because of the ability of such methods to elucidate mechanistic relationships (Runge et al., 2019). Methods that facilitate causal insights like information theory are applicable to many environmental timeseries with the advantage that they are model-free and not bound to linear assumptions (Wibral et al., 2013) and, in the case of transfer entropy, can account for strong autocorrelation in streamflow or solute concentrations. There has been debate about information theory's limitations for causal inferences in part due to the long data record lengths required for deriving probabilistic metrics (e.g., >500 points; Ruddell & Kumar, 2009) for the source and sink timeseries. There is potential for TE to over- or under-estimate causal interactions (James et al., 2016) or falsely convey synchrony if the source variable is closely correlated to an unmeasured "true" source of information (e.g., false positive). If the source and sink variables are synchronized at a timescale less than their measured frequency, the variables would exhibit no TE (e.g., false negative; Goodwell et al., 2020). However, these limitations are common in other causal inference methods, and we are confident that our analyses satisfy the requirements and assumptions of information theoretics.

Previous analyses exploring the relationship between wet deposition-river timeseries have primarily used correlative model structures. For example, numerous studies relate timeseries of wet deposition and river N by correlating the Sen slopes or Kendall tau of each variable, finding minimal evidence to suggest that stream N concentrations are related to depositional N concentrations (Argerich et al., 2013; Bernhardt et al., 2005; Goodale et al., 2003; Halliday et al., 2013). More recently, correlation coefficients were applied to long-term data sets to quantify the relationship between annual deposition and river N loads (Templer et al., 2022) with varying results. These methods assume that wet deposition-river synchrony is linear, temporally static and matched in time, all of which are in conflict with foundational biogeochemical theories such as nutrient spiraling (Ensign & Doyle, 2006), hot spots-hot moments (McClain et al., 2003), and the pulse-shunt hypothesis (Raymond et al., 2016). While advances in explaining deposition-river biogeochemical relationships using process-based (e.g., electrolyte solubility theory) models have been made (Monteith et al., 2023), lags in advection and biogeochemical processes have generally been unaccounted for in the deposition-watershed literature. Here we show accounting for lags and nonlinearity is achievable with non-linear and non-parametric approaches like information theory. Our study highlights the utility of such methods for quantifying lags between watershed N inputs and outputs while providing a connection to the body of work on the biogeochemistry of transient storage zones in watershed hydrology (Argerich et al., 2011; Claessens et al., 2010; Wollheim et al., 2014).

5. Conclusions

We used information theory to determine the potential fate of wet deposition N enroute to a receiving river. Overall, wet deposition N can reduce uncertainty of river N timeseries after accounting for antecedent river N conditions. Extending these analyses beyond their statistical definitions, we suggest that information theory results can facilitate causal inferences and the development of mechanistic hypotheses between driver (e.g., wet deposition) and response (e.g., river) variables. By applying information theory algorithms to timeseries of wet deposition N inputs and watershed N outputs, we produced hypotheses regarding plausible N cycling processes occurring within the Lamprey River watershed. We find that wet deposition-river pair-wise combinations indicative of assimilation and mineralization of N wet deposition displayed the highest degree of synchrony at lags of 12–21 weeks within the watershed. This study demonstrates that information theory is a powerful avenue for quantifying the degree to which wet deposition N influences river N chemistry. There are many promising potential applications of information theory to environmental timeseries. For example, extending the case study provided here to wet deposition and river N timeseries across a gradient of stream orders, watershed elevation, or watershed land use. Open-source tools, such as Hydrobench (Moges, Ruddell, Zhang, Driscoll, Norton, et al., 2022), provide resources for applying information-theoretic diagnostics to measure the flow of information among long-term or high-frequency timeseries variables. Such tools provide an opportunity to understand joint causal interactions between multiple source variables and one target variable (Goodwell & Bassiouni, 2022), for example, including timeseries from the terrestrial landscape (e.g., soil N or oxygen concentrations or soil saturation depth) as additional sources of information would illuminate the role of the watershed itself in modulating the synchrony between wet deposition and river N timeseries.

Data Availability Statement

The raw wet deposition and river chemistry, discharge, and precipitation data used for supporting the results presented in this paper are openly available on Hydroshare at https://doi.org/10.4211/hs.0d123f789d-3944f7a32aedc1fd4ea2e5 (Murray et al., 2023). The scripts used to run information theory algorithms were accessed and modified with permission from Moges, Ruddell, Zhang, Driscoll, and Larsen (2022) and Moges, Ruddell, Zhang, Driscoll, Norton, et al. (2022).

Acknowledgments

Support for DSM was provided by the NASA FINESST program (Grant 80NSSC1441). Funding for this project was also provided by the National Science Foundation (NSF) Experimental Program to Stimulate Competitive Research (EPSCoR) program awards EPS-1929148 (Canary in the Watershed) and EPS-1101245. Partial funding was provided by the New Hampshire Agriculture Experiment Station. This work was supported by the United Stated Department of Agriculture (USDA) National Institute of Food and Agriculture Hatch Multi-State Project 1022291 (ASW) and McIntire-Stennis project 1019522 (WHM). This is scientific contribution number 2961. Partial funding was also provided by the U.S. EPA through the Connecticut River Airshed-Watershed Consortium, the NH Water resources Research Center and the National Oceanic and Atmospheric Administration AIRMAP program. The authors acknowledge support from the University of New Hampshire CoRE program and the Watershed Informatics project.

References

Aber, J. D., Goodale, C. L., Ollinger, S. V., Smith, M. L., Magill, A. H., Martin, M. E., et al. (2003). Is nitrogen deposition altering the nitrogen status of northeastern forests? *BioScience*, *53*(4), 375–389. https://doi.org/10.1641/0006-3568

Aber, J. D., McDowell, W., Nadelhoffer, K., Magill, A., Berntson, G., McNulty, S., et al. (1998). Forest ecosystems hypotheses revisited. *BioScience*, *48*(11), 921–934. https://doi.org/10.2307/1313296

Ardón, M., Helton, A. M., Scheuerell, M. D., & Bernhardt, E. S. (2017). Fertilizer legacies meet saltwater incursion: Challenges and constraints for coastal plain wetland restoration. *Elementa: Science of the Anthropocene*, *5*, 41. https://doi.org/10.1525/elementa.236

Ardón, M., Morse, J. L., Colman, B. P., & Bernhardt, E. S. (2013). Drought-induced saltwater incursion leads to increased wetland nitrogen export. *Global Change Biology*, *19*(10), 2976–2985. https://doi.org/10.1111/gcb.12287

Argerich, A., Johnson, S. L., Sebestyen, S. D., Rhoades, C. C., Greathouse, E., Knoepp, J. D., et al. (2013). Trends in stream nitrogen concentrations for forested reference catchments across the USA. *Environmental Research Letters*, *8*(1), 014039. https://doi.org/10.1088/1748-9326/8/1/014039

Argerich, A., Martí, E., Sabater, F., Haggerty, R., & Ribot, M. (2011). Influence of transient storage on stream nutrient uptake based on substrata manipulation. *Aquatic Sciences*, *73*(3), 365–376. https://doi.org/10.1007/s00027-011-0184-9

Baron, J. S., Hall, E. K., Nolan, B. T., Finlay, J. C., Bernhardt, E. S., Harrison, J. A., et al. (2013). The interactive effects of excess reactive nitrogen and climate change on aquatic ecosystems and water resources of the United States. *Biogeochemistry*, *114*(1–3), 71–92. https://doi.org/10.1007/s10533-012-9788-y

Bastviken, D., Sandén, P., Svensson, T., Ståhlberg, C., Magounakis, M., & Öberg, G. (2006). Chloride retention and release in a boreal forest soil: Effects of soil water residence time and nitrogen and chloride loads. *Environmental Science & Technology*, *40*(9), 2977–2982. https://doi.org/10.1021/es0523237

Bennett, A., Nijssen, B., Ou, G., Clark, M., & Nearing, G. (2019). Quantifying process connectivity with transfer entropy in hydrologic models. *Water Resources Research*, *55*(6), 4613–4629. https://doi.org/10.1029/2018WR024555

Bernal, S., von Schiller, D., Martí, E., & Sabater, F. (2012). In-stream net uptake regulates inorganic nitrogen export from catchments under base flow conditions. *Journal of Geophysical Research*, *117*(G3), G00N05. https://doi.org/10.1029/2012JG001985

Bernhardt, E. S., Likens, G. E., Hall, R. O., Buso, D. C., Fisher, S. G., Burton, T. M., et al. (2005). Can't see the forest for the stream? In-stream processing and terrestrial nitrogen exports. *BioScience*, *55*(3), 219. https://doi.org/10.1641/0006-3568(2005)055[0219:ACSTFF]2.0.CO;2

Blöschl, G., & Sivapalan, M. (1995). Scale issues in hydrological modelling: A review. *Hydrological Processes*, *9*(3–4), 251–290. https://doi.org/10.1002/hyp.3360090305

Boyer, E. W., Hornberger, G. M., Bencala, K. E., & McKnight, D. M. (1997). Response characteristics of DOC flushing in an alpine catchment. *Hydrological Processes*, *11*(12), 1635–1647. https://doi.org/10.1002/(SICI)1099-1085(19971015)11:12<1635::AID-HYP494>3.0.CO;2-H

Brookshire, E. N. J., Valett, H. M., Thomas, S. A., & Webster, J. R. (2007). Atmospheric N deposition increases organic N loss from temperate forests. *Ecosystems*, *10*(2), 252–262. https://doi.org/10.1007/s10021-007-9019-x

Burt, T. P., & McDonnell, J. J. (2015). Whither field hydrology? The need for discovery science and outrageous hydrological hypotheses. *Water Resources Research*, *51*(8), 5919–5928. https://doi.org/10.1002/2014WR016839

Byrnes, D. K., Van Meter, K. J., & Basu, N. B. (2020). Long-term shifts in U.S. nitrogen sources and sinks revealed by the new TREND-nitrogen data set (1930–2017). *Global Biogeochemical Cycles*, *34*(9), 1–16. https://doi.org/10.1029/2020GB006626

Causse, J., BaurèS, E., Mery, Y., Jung, A.-V., & Thomas, O. (2015). Variability of N export in water: A review. *Critical Reviews in Environmental Science and Technology*, *45*(20), 2245–2281. https://doi.org/10.1080/10643389.2015.1010432

Chapman, T. G. (1986). Entropy as a measure of hydrologic data uncertainty and model performance. *Journal of Hydrology*, *85*(1–2), 111–126. https://doi.org/10.1016/0022-1694(86)90079-x

Chorover, J., Derry, L. A., & McDowell, W. H. (2017). Concentration-discharge relations in the critical zone: Implications for resolving critical zone structure, function, and evolution. *Water Resources Research*, *53*(11), 8654–8659. https://doi.org/10.1002/2017WR021111

Claessens, L., Tague, C. L., Groffman, P. M., & Melack, J. M. (2010). Longitudinal and seasonal variation of stream N uptake in an urbanizing watershed: Effect of organic matter, stream size, transient storage and debris dams. *Biogeochemistry*, *98*(1–3), 45–62. https://doi.org/10.1007/s10533-009-9375-z

Contosta, A. R., Adolph, A., Burchsted, D., Burakowski, E., Green, M., Guerra, D., et al. (2017). A longer vernal window: The role of winter coldness and snowpack in driving spring transitions and lags. *Global Change Biology*, *23*(4), 1610–1625. https://doi.org/10.1111/gcb.13517

Cornell, S. E. (2011). Atmospheric nitrogen deposition: Revisiting the question of the importance of the organic component. *Environmental Pollution*, *159*(10), 2214–2222. https://doi.org/10.1016/j.envpol.2010.11.014

Craine, J. M., Elmore, A. J., Wang, L., Aranibar, J., Bauters, M., Boeckx, P., et al. (2018). Isotopic evidence for oligotrophication of terrestrial ecosystems. *Nature Ecology & Evolution*, *2*(11), 1735–1744. https://doi.org/10.1038/s41559-018-0694-0

Creed, I. F., Hwang, T., Lutz, B., & Way, D. (2015). Climate warming causes intensification of the hydrological cycle, resulting in changes to the vernal and autumnal windows in a northern temperate forest. *Hydrological Processes*, *29*(16), 3519–3534. https://doi.org/10.1002/hyp.10450

Dunne, T. (1978). Field studies of hillslope flow processes. In M. J. Kirkby (Ed.) *Hillslope hydrology interaction of precipitation and streamflow* (pp. 227–293). John Wiley & Sons, Inc.

Durán, J., Morse, J. L., Groffman, P. M., Campbell, J. L., Christenson, L. M., Driscoll, C. T., et al. (2016). Climate change decreases nitrogen pools and mineralization rates in northern hardwood forests. *Ecosphere*, *7*(3), 1–13. https://doi.org/10.1002/ecs2.1251

Ensign, S. H., & Doyle, M. W. (2006). Nutrient spiraling in streams and river networks. *Journal of Geophysical Research*, *111*(4), 1–13. https://doi.org/10.1029/2005JG000114

Fazekas, H. M., McDowell, W. H., Shanley, J. B., & Wymore, A. S. (2021). Climate variability drives watersheds along a transporter-transformer continuum. *Geophysical Research Letters*, *48*(21), e2021GL094050. https://doi.org/10.1029/2021GL094050

Feng, X., Thompson, S. E., Woods, R., & Porporato, A. (2019). Quantifying asynchronicity of precipitation and potential evapotranspiration in Mediterranean climates. *Geophysical Research Letters*, *46*(24), 14692–14701. https://doi.org/10.1029/2019GL085653

Frades, M. C. (2008). Hydrologic analysis of the headwaters Lamprey River watershed using water isotopes. (Vol. *100*).

Franzen, S. E., Farahani, M. A., & Goodwell, A. E. (2020). Information flows: Characterizing precipitation-streamflow dependencies in the Colorado headwaters with an information theory approach. *Water Resources Research*, *56*(10), e2019WR026133. https://doi.org/10.1029/2019WR026133

Gilliam, F. S., Burns, D. A., Driscoll, C. T., Frey, S. D., Lovett, G. M., & Watmough, S. A. (2019). Decreased atmospheric nitrogen deposition in eastern North America: Predicted responses of forest ecosystems. *Environmental Pollution*, *244*, 560–574. https://doi.org/10.1016/j.envpol.2018.09.135

Gong, W., Yang, D., Gupta, H. V., & Nearing, G. (2014). Estimating information entropy for hydrological data: One-dimensional case. *Water Resources Research*, *50*(6), 5003–5018. https://doi.org/10.1002/2014WR015874

Goodale, C. L., Aber, J. D., & Vitousek, P. M. (2003). An unexpected nitrate decline in New Hampshire streams. *Ecosystems*, *6*(1), 0075–0086. https://doi.org/10.1007/s10021-002-0219-0

Goodwell, A. E., & Bassiouni, M. (2022). Source relationships and model structures determine information flow paths in ecohydrologic models. *Water Resources Research*, *58*(9), e2021WR031164. https://doi.org/10.1029/2021WR031164

Goodwell, A. E., Jiang, P., Ruddell, B. L., & Kumar, P. (2020). Debates—Does information theory provide a new paradigm for Earth science? Causality, interaction, and feedback. *Water Resources Research*, *56*(2), e2019WR024940. https://doi.org/10.1029/2019WR024940

Goodwell, A. E., & Kumar, P. (2017). Temporal information partitioning: Characterizing synergy, uniqueness, and redundancy in interacting environmental variables. *Water Resources Research*, *53*(7), 5920–5942. https://doi.org/10.1002/2016WR020216

Groffman, P. M., Driscoll, C. T., Durán, J., Campbell, J. L., Christenson, L. M., Fahey, T. J., et al. (2018). Nitrogen oligotrophication in northern hardwood forests. *Biogeochemistry*, *141*(3), 523–539. https://doi.org/10.1007/s10533-018-0445-y

Groffman, P. M., Driscoll, C. T., Fahey, T. J., Hardy, J. P., Fitzhugh, R. D., & Tierney, G. L. (2001). Colder soils in a warmer world: A snow manipulation study in a northern hardwood forest ecosystem. *Biogeochemistry*, *56*(2), 135–150. https://doi.org/10.1023/A:1013039830323

Halliday, S. J., Skeffington, R. A., Wade, A. J., Neal, C., Reynolds, B., Norris, D., & Kirchner, J. W. (2013). Upland streamwater nitrate dynamics across decadal to sub-daily timescales: A case study of Plynlimon, Wales. *Biogeosciences*, *10*(12), 8013–8038. https://doi.org/10.5194/bg-10-8013-2013

Herreid, A. M., Wymore, A. S., Varner, R. K., Potter, J. D., & McDowell, W. H. (2021). Divergent controls on stream greenhouse gas concentrations across a land-use gradient. *Ecosystems*, *24*(6), 1299–1316. https://doi.org/10.1007/s10021-020-00584-7

Hornberger, G. M., Bencala, K. E., & McKnight, D. M. (1994). Hydrological controls on dissolved organic carbon during snowmelt in the Snake River near Montezuma, Colorado. *Biogeochemistry*, *25*(3), 147–165. https://doi.org/10.1007/BF00024390

Hornberger, G. M., Scanlon, T. M., & Raffensperger, J. P. (2001). Modelling transport of dissolved silica in a forested headwater catchment: The effect of hydrological and chemical time scales on hysteresis in the concentration–discharge relationship. *Hydrological Processes*, *15*(10), 2029–2038.

James, R. G., Barnett, N., & Crutchfield, J. P. (2016). Information flows? A critique of transfer entropies. *Physical Review Letters*, *116*(23), 238701. https://doi.org/10.1103/PhysRevLett.116.238701

Jenkinson, D. S., Fox, R. H., & Rayner, J. H. (1985). Interactions between fertilizer nitrogen and soil nitrogen-the so-called 'priming' effect. *Journal of Soil Science*, *36*(3), 425–444. https://doi.org/10.1111/j.1365-2389.1985.tb00348.x

Kirchner, J. W. (2009). Catchments as simple dynamical systems: Catchment characterization, rainfall-runoff modeling, and doing hydrology backward. *Water Resources Research*, *45*(2), W02429. https://doi.org/10.1029/2008WR006912

Kirchner, J. W., Feng, X., & Neal, C. (2001). Catchment-scale advection and dispersion as a mechanism for fractal scaling in stream tracer concentrations. *Journal of Hydrology*, *254*(1–4), 82–101. https://doi.org/10.1016/S0022-1694(01)00487-5

Kirker, A. N., & Toran, L. (2023). Dual isotopes of nitrate reveal varying flow paths to stormwater retention basins. *Catena*, *220*, 106681. https://doi.org/10.1016/j.catena.2022.106681

Knuth, K. H., Gotera, A., Curry, C. T., Huyser, K. A., Wheeler, K. R., & Rossow, W. B. (2013). Revealing relationships among relevant climate variables with information theory. *(arXiv:1311.4632). arXiv*. http://arxiv.org/abs/1311.4632

Larsen, L. G., & Harvey, J. W. (2017). Disrupted carbon cycling in restored and unrestored urban streams: Critical timescales and controls: Disrupted carbon cycling in urban streams. *Limnology & Oceanography*, *62*(S1), S160–S182. https://doi.org/10.1002/lno.10613

Li, Z., Zeng, Z., Tian, D., Wang, J., Fu, Z., Zhang, F., et al. (2020). Global patterns and controlling factors of soil nitrification rate. *Global Change Biology*, *26*(7), 4147–4157. https://doi.org/10.1111/gcb.15119

Likens, G. E., & Bormann, F. H. (1974a). Acid rain: A serious regional environmental problem. *Science*, *184*(4142), 1176–1179. https://doi.org/10.1126/science.184.4142.1176

Likens, G. E., & Bormann, F. H. (1974b). Linkages between terrestrial and aquatic ecosystems. *BioScience*, *24*(8), 447–456. https://doi.org/10.2307/1296852

Liptzin, D., Boy, J., Campbell, J. L., Clarke, N., Laclau, J.-P., Godoy, R., et al. (2022). Spatial and temporal patterns in atmospheric deposition of dissolved organic carbon. *Global Biogeochemical Cycles*, *36*(10), e2022GB007393. https://doi.org/10.1029/2022GB007393

Liptzin, D., Daley, M. L., & McDowell, W. H. (2013). A comparison of wet deposition collectors at a coastal rural site. *Water, Air, & Soil Pollution*, *224*(5), 1558. https://doi.org/10.1007/s11270-013-1558-5

Lovett, G. M., Weathers, K. C., & Sobczak, W. V. (2000). Nitrogen saturation and retention in forested watersheds of the Catskill Mountains, New York. *Ecological Applications*, *10*(1), 73–84. https://doi.org/10.1890/1051-0761(2000)010[0073:NSARIF]2.0.CO;2

McClain, M. E., Boyer, E. W., Dent, C. L., Gergel, S. E., Grimm, N. B., Groffman, P. M., et al. (2003). Biogeochemical hot Spots and hot moments at the interface of terrestrial and aquatic ecosystems. *Ecosystems*, *6*(4), 301–312. https://doi.org/10.1007/s10021-003-0161-9

McDowell, W. H., Magill, A. H., Aitkenhead-Peterson, J. A., Aber, J. D., Merriam, J. L., & Kaushal, S. S. (2004). Effects of chronic nitrogen amendment on dissolved organic matter and inorganic nitrogen in soil solution. *Forest Ecology and Management*, *196*(1), 29–41. https://doi.org/10.1016/j.foreco.2004.03.010

Moges, E., Ruddell, B. L., Zhang, L., Driscoll, J. M., & Larsen, L. G. (2022). Strength and memory of precipitation's control over streamflow across the conterminous United States. *Water Resources Research*, *58*(3), e2021WR030186. https://doi.org/10.1029/2021WR030186

Moges, E., Ruddell, B. L., Zhang, L., Driscoll, J. M., Norton, P., Perez, F., & Larsen, L. G. (2022). HydroBench: Jupyter supported reproducible hydrological model benchmarking and diagnostic tool. *Frontiers in Earth Science*, *10*, 884766. https://doi.org/10.3389/feart.2022.884766

Monteith, D. T., Henrys, P. A., Hruška, J., de Wit, H. A., Krám, P., Moldan, F., et al. (2023). Long-term rise in riverine dissolved organic carbon concentration is predicted by electrolyte solubility theory. *Science Advances*, *9*(3), eade3491. https://doi.org/10.1126/sciadv.ade3491

Monteith, D. T., Stoddard, J. L., Evans, C. D., de Wit, H. A., Forsius, M., Høgåsen, T., et al. (2007). Dissolved organic carbon trends resulting from changes in atmospheric deposition chemistry. *Nature*, *450*(7169), 537–540. https://doi.org/10.1038/nature06316

Murdoch, P. S., & Stoddard, J. L. (1992). The role of nitrate in the acidification of streams in the Catskill Mountains of New York. *Water Resources Research*, *28*(10), 2707–2720. https://doi.org/10.1029/92WR00953

Murray, D., Wymore, A., McDowell, W. H., Potter, J., & Shattuck, M. (2023). Deposition and River paired timeseries [Dataset]. HydroShare. https://doi.org/10.4211/hs.8fbd7ea351754320a71d748043cbc4e8

Murray, D. S., Shattuck, M. D., McDowell, W. H., & Wymore, A. S. (2022). Nitrogen wet deposition stoichiometry: The role of organic nitrogen, seasonality, and snow. *Biogeochemistry*, *160*(3), 301–314. https://doi.org/10.1007/s10533-022-00966-0

Neitsch, S. L., Arnold, J. G., Kiniry, J. R., Williams, J. R., & King, K. W. (2001). Soil and water assessment tool theoretical documentation. *Blackland Research Center, Texas Agricultural Experiment Station*.

Newcomer, M. E., Bouskill, N. J., Wainwright, H., Maavara, T., Arora, B., Siirila-Woodburn, E. R., et al. (2021). Hysteresis patterns of watershed nitrogen retention and loss over the past 50 years in United States hydrological basins. *Global Biogeochemical Cycles*, *35*(4), 1–28. https://doi.org/10.1029/2020GB006777

Parton, W. J. (1996). The CENTURY model. In *Evaluation of soil organic matter models* (pp. 283–291). Springer. https://doi.org/10.1007/978-3-642-61094-3_23

Peterson, B. J., Wollheim, W. M., Mulholland, P. J., Webster, J. R., Meyer, J. L., Tank, J. L., et al. (2001). Control of nitrogen export from watersheds by headwater streams. *Science*, *292*(5514), 86–90. https://doi.org/10.1126/science.1056874

Quick, A. M., Reeder, W. J., Farrell, T. B., Tonina, D., Feris, K. P., & Benner, S. G. (2019). Nitrous oxide from streams and rivers: A review of primary biogeochemical pathways and environmental variables. *Earth-Science Reviews*, *191*, 224–262. https://doi.org/10.1016/j.earscirev.2019.02.021

Raymond, P. A., Saiers, J. E., & Sobczak, W. V. (2016). Hydrological and biogeochemical controls on watershed dissolved organic matter transport: Pulse-shunt concept. *Ecology*, *97*(1), 5–16. https://doi.org/10.1890/14-1684.1

Rinderer, M., Ali, G., & Larsen, L. G. (2018). Assessing structural, functional and effective hydrologic connectivity with brain neuroscience methods: State-of-the-art and research directions. *Earth-Science Reviews*, *178*, 29–47. https://doi.org/10.1016/j.earscirev.2018.01.009

Robertson, G. P., Sollins, P., Ellis, B. G., & Lajtha, K. (1999). Exchangeable ions, pH, and cation exchange capacity. In G. P. Robertson, C. S. Bledsoe, D. C. Coleman, & P. Sollins (Eds.), *Standard soil methods for long-term ecological research* (pp. 106–114). Oxford University Press.

Rodríguez-Cardona, B. M., Wymore, A. S., Argerich, A., Barnes, R. T., Bernal, S., Brookshire, E. N. J., et al. (2022). Shifting stoichiometry: Long-term trends in stream-dissolved organic matter reveal altered C:N ratios due to history of atmospheric acid deposition. *Global Change Biology*, *28*(1), 98–114. https://doi.org/10.1111/gcb.15965

Ruddell, B. L., & Kumar, P. (2009). Ecohydrologic process networks: 1. Identification: Ecohydrologic process networks, 1. *Water Resources Research*, *45*(3), W03419. https://doi.org/10.1029/2008WR007279

Runge, J., Bathiany, S., Bollt, E., Camps-Valls, G., Coumou, D., Deyle, E., et al. (2019). Inferring causation from timeseries in Earth system sciences. *Nature Communications*, *10*(1), 2553. https://doi.org/10.1038/s41467-019-10105-3

Schreiber, T. (2000). Measuring information transfer. *Physical Review Letters*, *85*(2), 461–464. https://doi.org/10.1103/PhysRevLett.85.461

Seybold, E. C., Dwivedi, R., Musselman, K. N., Kincaid, D. W., Schroth, A. W., Classen, A. T., et al. (2022). Winter runoff events pose an unquantified continental-scale risk of high wintertime nutrient export. *Environmental Research Letters*, *17*(10), 104044. https://doi.org/10.1088/1748-9326/ac8be5

Seybold, E. C., Fork, M. L., Braswell, A. E., Blaszczak, J. R., Fuller, M. R., Kaiser, K. E., et al. (2022). A classification framework to assess ecological, biogeochemical, and hydrologic synchrony and asynchrony. *Ecosystems*, *25*(5), 989–1005. https://doi.org/10.1007/s10021-021-00700-1

Shannon, C. (1949). The mathematical theory of communication. In C. Shannon, & W. Weaver (Eds.), *The mathematical theory of communication*. University of Illinois Press.

Sivapalan, M., Jothityangkoon, C., & Menabde, M. (2002). Linearity and nonlinearity of basin response as a function of scale: Discussion of alternative definitions: Technical Note. *Water Resources Research*, *38*(2), 4–5. https://doi.org/10.1029/2001WR000482

Smith, P., Smith, J. U., Powlson, D. S., Mcgill, W. B., Arah, J. R. M., Chertov, O. G., et al. (1997). A comparison of the performance of nine soil organic matter models using datasets from seven long-term experiments. *Geoderma*, *81*(1–2), 153–225. https://doi.org/10.1016/S0016-7061(97)00087-6

Strauss, E. A., & Lamberti, G. A. (2000). Regulation of nitrification in aquatic sediments by organic carbon. *Limnology & Oceanography*, *45*(8), 1854–1859. https://doi.org/10.4319/lo.2000.45.8.1854

Strauss, E. A., & Lamberti, G. A. (2002). Effect of dissolved organic carbon quality on microbial decomposition and nitrification rates in stream sediments. *Freshwater Biology*, *47*(1), 65–74. https://doi.org/10.1046/j.1365-2427.2002.00776.x

Sturtevant, C., Ruddell, B. L., Knox, S. H., Verfaillie, J., Matthes, J. H., Oikawa, P. Y., & Baldocchi, D. (2016). Identifying scale-emergent, nonlinear, asynchronous processes of wetland methane exchange. *Journal of Geophysical Research: Biogeosciences*, *121*(1), 188–204. https://doi.org/10.1002/2015JG003054

Templer, P. H., Harrison, J. L., Pilotto, F., Flores-Díaz, A., Haase, P., McDowell, W. H., et al. (2022). Atmospheric deposition and precipitation are important predictors of inorganic nitrogen export to streams from forest and grassland watersheds: A large-scale data synthesis. *Biogeochemistry*, *160*(2), 219–241. https://doi.org/10.1007/s10533-022-00951-7

Tennant, C., Larsen, L., Bellugi, D., Moges, E., Zhang, L., & Ma, H. (2020). The utility of information flow in formulating discharge forecast models: A case study from an arid snow-dominated catchment. *Water Resources Research*, *56*(8), e2019WR024908. https://doi.org/10.1029/2019WR024908

Triska, F. J., Jackman, A. P., Duff, J. H., & Avanzino, R. J. (1994). Ammonium sorption to channel and riparian sediments: A transient storage pool for dissolved inorganic nitrogen. *Biogeochemistry*, *26*(2), 67–83. https://doi.org/10.1007/bf02182880

Vannote, R. L., Minshall, G. W., Cummins, K. W., Sedell, J. R., & Cushing, C. E. (1980). The river continuum concept. *Canadian Journal of Fisheries and Aquatic Sciences*, *37*(1), 130–137. https://doi.org/10.1139/f80-017

Whitehead, P. G., Wilby, R. L., Battarbee, R. W., Kernan, M., & Wade, A. J. (2009). A review of the potential impacts of climate change on surface water quality. *Hydrological Sciences Journal*, *54*(1), 101–123. https://doi.org/10.1623/hysj.54.1.101

Wibral, M., Pampu, N., Priesemann, V., Siebenhühner, F., Seiwert, H., Lindner, M., et al. (2013). Measuring information-transfer delays. *PLoS One*, *8*(2), e55809. https://doi.org/10.1371/journal.pone.0055809

Wollheim, W. M., Harms, T. K., Peterson, B. J., Morkeski, K., Hopkinson, C. S., Stewart, R. J., & Briggs, M. A. (2014). Nitrate uptake dynamics of surface transient storage in stream channels and fluvial wetlands. *Biogeochemistry*, *120*(1–3), 239–257. https://doi.org/10.1007/s10533-014-9993-y

Wu, S., Zhao, J., Wang, H., & Sivapalan, M. (2021). Regional patterns and physical controls of streamflow generation across the conterminous United States. *Water Resources Research*, *57*(6), e2020WR028086. https://doi.org/10.1029/2020WR028086

Wymore, A. S., Rodríguez-Cardona, B., & McDowell, W. H. (2015). Direct response of dissolved organic nitrogen to nitrate availability in headwater streams. *Biogeochemistry*, *126*(1–2), 1–10. https://doi.org/10.1007/s10533-015-0153-9

Wymore, A. S., Shattuck, M. D., Potter, J. D., Snyder, L., & McDowell, W. H. (2021). The Lamprey River Hydrological Observatory: Suburbanization and changing seasonality. *Hydrological Processes*, *35*(4). https://doi.org/10.1002/hyp.14131

Zuidema, S. (2011). Identifying groundwater contributions to baseflow in a temperate headwater catchment. Master's Theses and Capstones. Retrieved from https://scholars.unh.edu/thesis/647